

1 **Mitochondrial respiratory states and rates:**  
2 **Building blocks of mitochondrial physiology**

3 Part 1. MitoEAGLE preprint 2018-02-28(31)

4  
5 [http://www.mito eagle.org/index.php/MitoEAGLE\\_preprint\\_2018-02-08](http://www.mito eagle.org/index.php/MitoEAGLE_preprint_2018-02-08)

6 Preprint version 31 (2018-02-28)

7  
8 **MitoEAGLE Network**

9 Corresponding author: Gnaiger E

10 Co-authors:

11 Aasander Frostner E, Acuna-Castroviejo D, Ahn B, Alves MG, Amati F, Aral C,  
12 Arandarčkaitė O, Bailey DM, Bakker BM, Bastos Sant'Anna Silva AC, Battino M, Beard  
13 DA, Ben-Shachar D, Bishop D, Borsheim E, Borutaitė V, Breton S, Brown GC, Brown RA,  
14 Buettner GR, Burtscher J, Calabria E, Calbet JA, Calzia E, Cardoso LHD, Carvalho E,  
15 Casado Pinna M, Cervinkova Z, Chang SC, Chaurasia B, Chen Q, Chicco AJ, Chinopoulos C,  
16 Clementi E, Coen PM, Collin A, Crisóstomo L, Das AM, Davis MS, De Palma C, Dias TR,  
17 Distefano G, Doerrier C, Drahota Z, Duchon MR, Durham WJ, Ehinger J, Elmer E, Endlicher  
18 R, Fell DA, Ferko M, Ferreira JCB, Ferreira R, Filipovska A, Fisar Z, Fischer M, Fisher JJ,  
19 Fornaro M, Galkin A, Garcia-Roves PM, Garcia-Souza LF, Garten A, Genova ML, Giovarelli  
20 M, Gonzalez-Armenta JL, Gonzalo H, Goodpaster BH, Gorr TA, Gourlay CW, Granata C,  
21 Grefte S, Haas CB, Haavik J, Han J, Harrison DK, Hellgren KT, Hernansanz-Agustin P,  
22 Holland OJ, Hoppel CL, Houstek J, Hunger M, Iglesias-Gonzalez J, Irving BA, Iyer S,  
23 Jackson CB, Jadiya P, Jang DH, Jansen-Dürr P, Jespersen NR, Jha RK, Kaambre T, Kane  
24 DA, Kappler L, Karabatsiakakis A, Keijer J, Keppner G, Khamoui AV, Klingenspor M,  
25 Komlodi T, Koopman WJH, Kopitar-Jerala N, Krako Jakovljevic N, Kuang J, Kucera O,  
26 Labieniec-Watala M, Lai N, Laner V, Larsen TS, Lee HK, Leeuwenburgh C, Lemieux H,  
27 Lerfall J, Liu J, Lucchinetti E, MacMillan-Crow LA, Makrecka-Kuka M, Malik A, Markova  
28 M, Meszaros AT, Michalak S, Moiso N, Molina AJA, Montaigne D, Moore AL, Moreira BP,  
29 Mracek T, Muntane J, Muntean DM, Murray AJ, Nemec M, Neuzil J, Newsom S, Nozickova  
30 K, O'Gorman D, Oliveira MT, Oliveira PF, Oliveira PJ, Orynbayeva Z, Pak YK, Palmeira  
31 CM, Patel HH, Pecina P, Pelena D, Pereira da Silva Grilo da Silva F, Pesta D, Petit PX,  
32 Pichaud N, Piel S, Pirkmajer S, Porter RK, Pranger F, Prochownik EV, Pulinilkunnit T,  
33 Puurand M, Radenkovic F, Radi R, Ramzan R, Reboredo P, Renner-Sattler K, Robinson MM,  
34 Rohlena J, Rolo AP, Ropelle ER, Røslund GV, Rossiter HB, Rybacka-Mossakowska J, Saada  
35 A, Safaei Z, Salvadego D, Sandi C, Scatena R, Schartner M, Scheibye-Knudsen M, Schilling  
36 JM, Schlattner U, Schönfeld P, Schwarzer C, Scott GR, Shabalina IG, Sharma P, Sharma V,  
37 Shevchuk I, Siewiera K, Silber AM, Singer D, Smenes BT, Soares FAA, Sobotka O,  
38 Sokolova I, Spinazzi M, Stankova P, Stier A, Stocker R, Sumbalova Z, Suravajhala P,  
39 Swerdlow RH, Swiniuch D, Tanaka M, Tandler B, Tavernarakis N, Tepp K, Thyfault JP,  
40 Tomar D, Towheed A, Tretter L, Trifunovic A, Trivigno C, Tronstad KJ, Trougakos IP,  
41 Tyrrell DJ, Urban T, Valentine JM, Velika B, Vendelin M, Vercesi AE, Victor VM, Villena  
42 JA, Vitorino RMP, Vogt S, Volani C, Votion DM, Vujacic-Mirski K, Wagner BA, Ward ML,  
43 Watala C, Wei YH, Wieckowski MR, Williams C, Wohlwend M, Wolff J, Wuest RCI, Zaugg  
44 K, Zaugg M, Zischka H, Zorzano A

45  
46 Supporting:

47 Bernardi P, Boetker HE, Bouitbir J, Coker RH, Dubouchaud H, Dyrstad SE, Engin AB, Gan  
48 Z, Garlid KD, Haendeler J, Hand SC, Hepple RT, Hickey AJ, Hoel F, Kainulainen H,  
49 Kowaltowski AJ, Krajcova A, Lane N, Lenaz G, Liu SS, Mazat JP, Menze MA, Methner A,  
50 Nedergaard J, Pallotta ML, Parajuli N, Pettersen IK, Porter C, Salin K, Sazanov LA, Skolik  
51 R, Sonkar VK, Szabo I, Vieyra A

**Updates and discussion:**

[http://www.mitoeagle.org/index.php/MitoEAGLE\\_preprint\\_2018-02-08](http://www.mitoeagle.org/index.php/MitoEAGLE_preprint_2018-02-08)

Correspondence: Gnaiger E

*Chair COST Action CA15203 MitoEAGLE* – <http://www.mitoeagle.org>

*Department of Visceral, Transplant and Thoracic Surgery, D. Swarovski Research  
Laboratory, Medical University of Innsbruck, Innrain 66/4, A-6020 Innsbruck, Austria*

*Email: mitoeagle@i-med.ac.at*

*Tel: +43 512 566796, Fax: +43 512 566796 20*

**Contents****Abstract****Executive summary****1. Introduction** – Box 1: In brief: Mitochondria and Bioblasts**2. Oxidative phosphorylation and coupling states in mitochondrial preparations**

Mitochondrial preparations

*2.1. Respiratory control and coupling*

The steady-state

Specification of biochemical dose

Phosphorylation,  $P_{\gg}$ , and  $P_{\gg}/O_2$  ratio

Control and regulation

Respiratory control and response

Respiratory coupling control and ET-pathway control

Coupling

Uncoupling

*2.2. Coupling states and respiratory rates*

Respiratory capacities in coupling control states

LEAK, OXPHOS, ET, ROX

Quantitative relations

*2.3. Classical terminology for isolated mitochondria*

States 1–5

**3. Normalization: fluxes and flows***3.1. Normalization: system or sample*

Flow per system,  $I$

Extensive quantities

Size-specific quantities – Box 2: Metabolic fluxes and flows: vectorial and scalar

*3.2. Normalization for system-size: flux per chamber volume*

System-specific flux,  $J_{V,O_2}$

*3.3. Normalization: per sample*

Sample concentration,  $C_{mX}$

Mass-specific flux,  $J_{O_2/mX}$

Number concentration,  $C_{NX}$

Flow per object,  $I_{O_2/X}$

*3.4. Normalization for mitochondrial content*

Mitochondrial concentration,  $C_{mtE}$ , and mitochondrial markers

Mitochondria-specific flux,  $J_{O_2/mtE}$

*3.5. Evaluation of mitochondrial markers**3.6. Conversion: units***4. Conclusions** – Box 3: Definitions: Mitochondrial and cell respiration**5. References**

103 **Abstract** As the knowledge base and importance of mitochondrial physiology to human health  
104 expands, the necessity for harmonizing nomenclature concerning mitochondrial respiratory  
105 states and rates has become increasingly apparent. Clarity of concept and consistency of  
106 nomenclature are key trademarks of a research field. These features facilitate effective  
107 transdisciplinary communication, education, and ultimately further discovery. The  
108 chemiosmotic theory establishes the mechanism of energy transformation and coupling in  
109 oxidative phosphorylation. The unifying concept of the protonmotive force provides the  
110 framework for developing a consistent theoretical foundation of mitochondrial physiology and  
111 bioenergetics. We follow IUPAC guidelines on terminology in physical chemistry, extended  
112 by considerations on open systems and irreversible thermodynamics. The concept-driven  
113 constructive terminology incorporates the meaning of each quantity and aligns concepts and  
114 symbols to the nomenclature of classical bioenergetics. In the frame of COST Action  
115 MitoEAGLE open to global bottom-up input, we endeavour to provide a balanced view on  
116 mitochondrial respiratory control and a critical discussion on reporting data of mitochondrial  
117 respiration in terms of metabolic flows and fluxes. Uniform standards for evaluation of  
118 respiratory states and rates will ultimately support the development of databases of  
119 mitochondrial respiratory function in species, tissues, and cells.

120

121 *Keywords:* Mitochondrial respiratory control, coupling control, mitochondrial  
122 preparations, protonmotive force, uncoupling, oxidative phosphorylation, OXPHOS,  
123 efficiency, electron transfer, ET; proton leak, LEAK, residual oxygen consumption, ROX, State  
124 2, State 3, State 4, normalization, flow, flux, O<sub>2</sub>

125

126

127

---

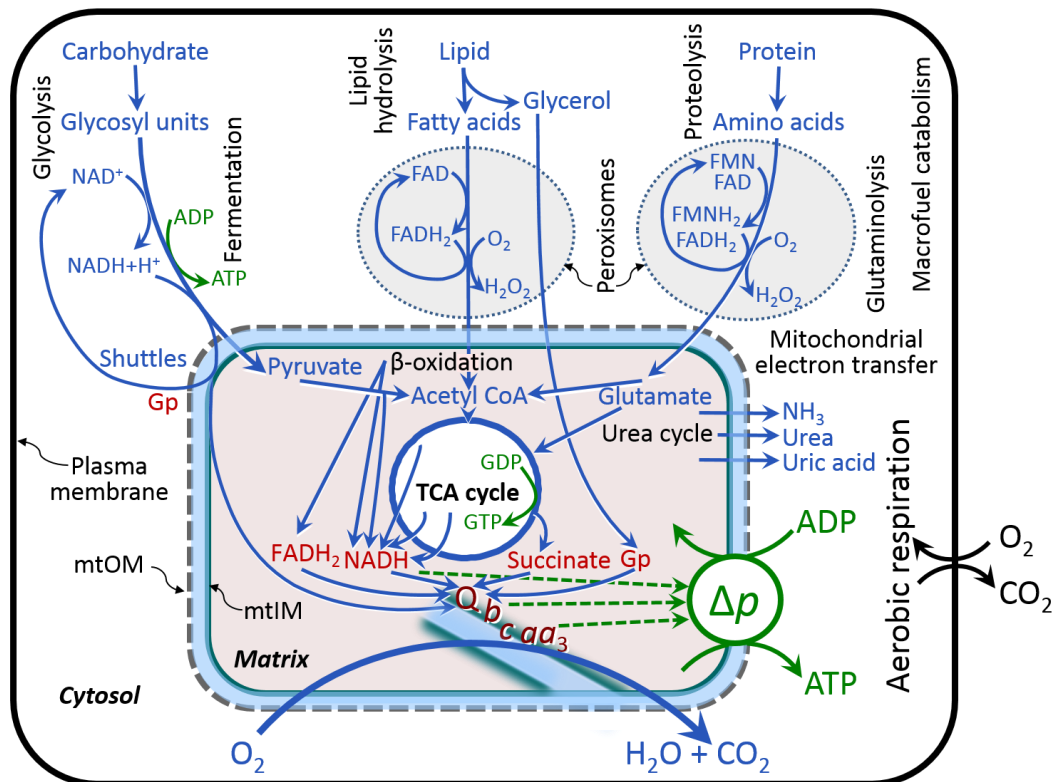
## 128 **Executive summary**

129

- 130 1. In view of broad implications on health care, mitochondrial researchers face an  
131 increasing responsibility to disseminate their fundamental knowledge and novel  
132 discoveries to a wide range of stakeholders and scientists beyond the group of  
133 specialists. This requires implementation of a commonly accepted terminology  
134 within the discipline and standardization in the translational context. Authors,  
135 reviewers, journal editors, and lecturers are challenged to collaborate with the aim  
136 to harmonize the nomenclature in the growing field of mitochondrial physiology  
137 and bioenergetics.
- 138 2. Aerobic energy metabolism in mitochondria of most eukaryotic cells depends on the  
139 coupling of phosphorylation ( $\text{ADP} \rightarrow \text{ATP}$ ) to O<sub>2</sub> flux in catabolic reactions. In the  
140 process of oxidative phosphorylation, coupling is mediated by translocation of  
141 protons through respiratory proton pumps operating across the inner mitochondrial  
142 membrane and generating or utilizing the protonmotive force measured between  
143 the mitochondrial matrix and intermembrane compartment. Compartmental  
144 coupling distinguishes vectorial oxidative phosphorylation from fermentation as the  
145 counterpart of cellular core energy metabolism (**Figure 1**).
- 146 3. To exclude fermentation and other cytosolic interactions from exerting an effect on  
147 mitochondrial metabolism, the barrier function of the plasma membrane must be  
148 disrupted. Selective removal or permeabilization of the plasma membrane yields  
149 mitochondrial preparations—including isolated mitochondria, tissue and cellular  
150 preparations—with structural and functional integrity. Then extra-mitochondrial  
151 concentrations of fuel substrates transported into the mitochondrial matrix, ADP,  
152 ATP, inorganic phosphate, and cations including H<sup>+</sup> can be controlled to determine  
153 mitochondrial function under a set of conditions defined as coupling control states.

154  
155  
156  
157

A concept-driven terminology of bioenergetics incorporates in its terms and symbols explicit information on the nature of respiratory states, that makes the technical terms readily recognized and easy to understand.



158  
159  
160  
161  
162  
163  
164  
165  
166  
167  
168  
169  
170  
171  
172  
173  
174  
175  
176  
177  
178  
179  
180  
181  
182  
183

**Figure 1. Mitochondrial respiration in the framework of cellular catabolism**

Mitochondrial respiration is the utilization of fuel substrates, which are the products of extra-mitochondrial catabolism of macrofuels or are taken up by the cell as small molecules, for electron transfer to  $O_2$  as the electron acceptor. Many fuel substrates are catabolized to acetyl-Co or glutamate, and further electron transfer reduces nicotinamide adenine dinucleotide to NADH or flavin adenine dinucleotide to  $FADH_2$ . In aerobic respiration, electron transfer is coupled to the phosphorylation of ADP to ATP, with energy transformation mediated by the protonmotive force,  $\Delta p$ . Anabolic reactions are tightly integrated with catabolism, both by ATP as the intermediary energy currency and by small organic precursor molecules as building blocks for biosynthesis (not shown). Glycolysis involves substrate-level phosphorylation of ADP to ATP in fermentation without utilization of  $O_2$ . In contrast, extra-mitochondrial oxidation of fatty acids and amino acids proceeds partially in peroxisomes without coupling to ATP production: acyl-CoA oxidase catalyzes the oxidation of  $FADH_2$  with electron transfer to  $O_2$ ; amino acid oxidases oxidize flavin mononucleotide  $FMNH_2$  or  $FADH_2$ . Coenzyme Q, Q, and the cytochromes *b*, *c*, and *aa<sub>3</sub>* are redox systems of the mitochondrial inner membrane, mtIM. Dashed arrows indicate the connection between the redox proton pumps (respiratory Complexes CI, CIII and CIV) and the transmembrane  $\Delta p$ . Mitochondrial outer membrane, mtOM; glycerol-3-phosphate, Gp; tricarboxylic acid cycle, TCA cycle.

4. Mitochondrial coupling states are defined according to the control of respiratory oxygen flux by the protonmotive force. Capacities of oxidative phosphorylation and electron transfer are measured at kinetically saturating concentrations of fuel substrates, ADP and inorganic phosphate, or at optimal uncoupler concentrations, respectively. Respiratory capacities are a measure of the upper bound of the rates of respiration, providing reference values for the diagnosis of health and disease,

- 184 and for evaluation of the effects of **E**volutionary background, **A**ge, **G**ender and sex,  
 185 **L**ifestyle and **E**nvironment (EAGLE).
- 186 5. Some degree of uncoupling is a characteristic of energy-transformations across  
 187 membranes. Uncoupling is caused by a variety of physiological, pathological,  
 188 toxicological, pharmacological and environmental conditions that exert an  
 189 influence not only on the proton leak and cation cycling, but also on proton slip  
 190 within the proton pumps and the structural integrity of the mitochondria. A more  
 191 loosely coupled state is induced by stimulation of mitochondrial superoxide  
 192 formation and the bypass of proton pumps. In addition, uncoupling by application  
 193 of protonophores represents an experimental intervention for the transition from a  
 194 well-coupled to the noncoupled state of mitochondrial respiration.
  - 195 6. Respiratory oxygen consumption rates have to be carefully normalized to enable meta-  
 196 analytic studies beyond the specific question of a particular experiment. Therefore,  
 197 all raw data should be published in a supplemental table or open access data  
 198 repository. Normalization of rates for the volume of the experimental chamber (the  
 199 measuring system) is distinguished from normalization for (1) the volume or mass  
 200 of the experimental sample, (2) the number of objects (cells, organisms), and (3)  
 201 the concentration of mitochondrial markers in the chamber.
  - 202 7. The consistent use of terms and symbols will facilitate transdisciplinary communication  
 203 and support further developments of a database on bioenergetics and mitochondrial  
 204 physiology. The present considerations are focused on studies with mitochondrial  
 205 preparations. These will be extended in a series of reports on pathway control of  
 206 mitochondrial respiration, the protonmotive force, respiratory states in intact cells,  
 207 and harmonization of experimental procedures.

---

### 212 **Box 1: In brief – Mitochondria and Bioblasts**

214 **Mitochondria** are the oxygen-consuming electrochemical generators evolved from  
 215 endosymbiotic bacteria (Margulis 1970; Lane 2005). They were described by Richard Altmann  
 216 (1894) as ‘bioblasts’, which include not only the mitochondria as presently defined, but also  
 217 symbiotic and free-living bacteria. The word ‘mitochondria’ (Greek mitos: thread; chondros:  
 218 granule) was introduced by Carl Benda (1898).

219 Mitochondria are dynamic networks contained within eukaryotic cells morphologically  
 220 characterized by a double membrane. The mitochondrial inner membrane (mtIM) shows  
 221 dynamic tubular to disk-shaped cristae that separate the mitochondrial matrix, *i.e.*, the  
 222 negatively charged internal mitochondrial compartment, from the intermembrane space; the  
 223 latter being positively charged and enclosed by the mitochondrial outer membrane (mtOM).  
 224 The mtIM contains the non-bilayer phospholipid cardiolipin, which is not present in any other  
 225 eukaryotic cellular membrane. Cardiolipin promotes the formation of respiratory  
 226 supercomplexes (SC I<sub>n</sub>III<sub>n</sub>IV<sub>n</sub>), which are supramolecular assemblies based upon specific,  
 227 though dynamic interactions between individual respiratory complexes (Greggio *et al.* 2017;  
 228 Lenaz *et al.* 2017). Membrane fluidity exerts an influence on functional properties of proteins  
 229 incorporated in the membranes (Waczulikova *et al.* 2007). In addition to mitochondrial  
 230 movement along microtubules, mitochondrial morphology can change in response to energy  
 231 requirements of the cell via processes known as fusion and fission, through which mitochondria  
 232 communicate within a network, and in response to intracellular stress factors causing swelling  
 233 and ultimately permeability transition.



234 Mitochondria are the structural and functional elements of cell respiration. Mitochondrial  
235 respiration is the reduction of oxygen by electron transfer coupled to electrochemical proton  
236 translocation across the mtIM. In the process of oxidative phosphorylation (OXPHOS), the  
237 catabolic reaction of oxygen consumption is electrochemically coupled to the transformation of  
238 energy in the form of adenosine triphosphate (ATP; Mitchell 1961, 2011). Mitochondria are the  
239 powerhouses of the cell which contain the machinery of the OXPHOS-pathways, including  
240 transmembrane respiratory complexes (proton pumps with FMN, Fe-S and cytochrome *b*, *c*,  
241 *aa<sub>3</sub>* redox systems); alternative dehydrogenases and oxidases; the coenzyme ubiquinone (Q);  
242 F-ATPase or ATP synthase; the enzymes of the tricarboxylic acid cycle, fatty acid and  
243 aminoacid oxidation; transporters of ions, metabolites and co-factors; and mitochondrial  
244 kinases related to energy transfer pathways. The mitochondrial proteome comprises over 1,200  
245 proteins (Calvo *et al.* 2015; 2017), mostly encoded by nuclear DNA (nDNA), with a variety of  
246 functions, many of which are relatively well known (*e.g.*, proteins regulating mitochondrial  
247 biogenesis or apoptosis), while others are still under investigation, or need to be identified (*e.g.*,  
248 alanine transporter).

249 There is a constant crosstalk between mitochondria and the other cellular components.  
250 The crosstalk between mitochondria and endoplasmic reticulum is involved in the regulation of  
251 calcium homeostasis, cell division, autophagy, differentiation, anti-viral signaling (Murley and  
252 Nunnari 2016). Mitochondria contribute to the formation of peroxisomes, which are hybrids of  
253 mitochondrial and ER-derived precursors (Sugiura *et al.* 2017). Cellular mitochondrial  
254 homeostasis (mitostasis) is maintained through regulation at both the transcriptional and post-  
255 translational level. Cell signalling modules contribute to homeostatic regulation throughout the  
256 cell cycle or even cell death by activating proteostatic modules (*e.g.*, the ubiquitin-proteasome  
257 and autophagy-lysosome pathways) and genome stability modules in response to varying  
258 energy demands and stress cues (Quiros *et al.* 2016).

259 Mitochondria typically maintain several copies of their own genome known as  
260 mitochondrial DNA (mtDNA; hundred to thousands per cell; Cummins 1998), which is  
261 maternally inherited. Biparental mitochondrial inheritance is documented in mammals, birds,  
262 fish, reptiles and invertebrate groups, and is even the norm in bivalves (Breton *et al.* 2007;  
263 White *et al.* 2008). mtDNA is compact (16.5 kB in humans) and encodes 13 protein subunits  
264 of the transmembrane respiratory Complexes CI, CIII, CIV and F-ATPase, 22 tRNAs, and two  
265 RNAs. Additional gene content has been suggested to include microRNAs, piRNA,  
266 smithRNAs, repeat associated RNA, and even additional proteins (Duarte *et al.* 2014; Lee *et al.*  
267 *et al.* 2015; Cobb *et al.* 2016). The mitochondrial genome requires nuclear-encoded  
268 mitochondrially targeted proteins for its maintenance and expression (Rackham *et al.* 2012).

269 Mitochondrial dysfunction is associated with a wide variety of genetic and degenerative  
270 diseases. Robust mitochondrial function is supported by physical exercise and caloric balance,  
271 and is central for sustained metabolic health throughout life. Therefore, a more consistent  
272 presentation of mitochondrial physiology will improve our understanding of the etiology of  
273 disease, the diagnostic repertoire of mitochondrial medicine, with a focus on protective  
274 medicine, lifestyle and healthy aging.

275 Abbreviation: mt, as generally used in mtDNA. Mitochondrion is singular and  
276 mitochondria is plural.

277 *‘For the physiologist, mitochondria afforded the first opportunity for an experimental*  
278 *approach to structure-function relationships, in particular those involved in active transport,*  
279 *vectorial metabolism, and metabolic control mechanisms on a subcellular level’* (Ernster and  
280 Schatz 1981).

281

282

283

284

## 285 1. Introduction

286

287 Mitochondria are the powerhouses of the cell with numerous physiological, molecular,  
 288 and genetic functions (**Box 1**). Every study of mitochondrial health and disease is faced with  
 289 **E**volution, **A**ge, **G**ender and sex, **L**ifestyle, and **E**nvironment (EAGLE) as essential background  
 290 conditions intrinsic to the individual patient or subject, cohort, species, tissue and to some extent  
 291 even cell line. As a large and coordinated group of laboratories and researchers, the mission of  
 292 the global MitoEAGLE Network is to generate the necessary scale, type, and quality of  
 293 consistent data sets and conditions to address this intrinsic complexity. Harmonization of  
 294 experimental protocols and implementation of a quality control and data management system  
 295 are required to interrelate results gathered across a spectrum of studies and to generate a  
 296 rigorously monitored database focused on mitochondrial respiratory function. In this way,  
 297 researchers within the same and across different disciplines can compare findings across  
 298 traditions and generations to clearly defined and accepted international standards.

299 Reliability and comparability of quantitative results depend on the accuracy of  
 300 measurements under strictly-defined conditions. A conceptual framework is required to warrant  
 301 meaningful interpretation and comparability of experimental outcomes carried out by research  
 302 groups at different institutes. With an emphasis on quality of research, collected data can be  
 303 useful far beyond the specific question of a particular experiment. Enabling meta-analytic  
 304 studies is the most economic way of providing robust answers to biological questions (Cooper  
 305 *et al.* 2009). Vague or ambiguous jargon can lead to confusion and may relegate valuable  
 306 signals to wasteful noise. For this reason, measured values must be expressed in standard units  
 307 for each parameter used to define mitochondrial respiratory function. Harmonization of  
 308 nomenclature and definition of technical terms are essential to improve the awareness of the  
 309 intricate meaning of current and past scientific vocabulary, for documentation and integration  
 310 into databases in general, and quantitative modelling in particular (Beard 2005). The focus on  
 311 coupling states and fluxes through metabolic pathways of aerobic energy transformation in  
 312 mitochondrial preparations is a first step in the attempt to generate a conceptually-oriented  
 313 nomenclature in bioenergetics and mitochondrial physiology. Coupling states of intact cells,  
 314 the protonmotive force, and respiratory control by fuel substrates and specific inhibitors of  
 315 respiratory enzymes will be reviewed in subsequent communications.

316

317

## 318 2. Oxidative phosphorylation and coupling states in mitochondrial preparations

319 *‘Every professional group develops its own technical jargon for talking about matters of*  
 320 *critical concern ... People who know a word can share that idea with other members of*  
 321 *their group, and a shared vocabulary is part of the glue that holds people together and*  
 322 *allows them to create a shared culture’ (Miller 1991).*

323

324 **Mitochondrial preparations** are defined as either isolated mitochondria, or tissue and  
 325 cellular preparations in which the barrier function of the plasma membrane is disrupted. Since  
 326 this entails the loss of cell viability, mitochondrial preparations are not studied *in vivo*. In  
 327 contrast to isolated mitochondria and tissue homogenate preparations, mitochondria in  
 328 permeabilized tissues and cells are *in situ* relative to the plasma membrane. The plasma  
 329 membrane separates the intracellular compartment including the cytosol, nucleus, and  
 330 organelles from the environment of the cell. The plasma membrane consists of a lipid bilayer  
 331 with embedded proteins and attached organic molecules that collectively control the selective  
 332 permeability of ions, organic molecules, and particles across the cell boundary. The intact  
 333 plasma membrane prevents the passage of many water-soluble mitochondrial substrates and  
 334 inorganic ions—such as succinate, adenosine diphosphate (ADP) and inorganic phosphate (P<sub>i</sub>),  
 335 that must be controlled at kinetically-saturating concentrations for the analysis of respiratory

336 capacities; this limits the scope of investigations into mitochondrial respiratory function in  
337 intact cells.

338 The cholesterol content of the plasma membrane is high compared to mitochondrial  
339 membranes. Therefore, mild detergents—such as digitonin and saponin—can be applied to  
340 selectively permeabilize the plasma membrane by interaction with cholesterol and allow free  
341 exchange of organic molecules and inorganic ions between the cytosol and the immediate cell  
342 environment, while maintaining the integrity and localization of organelles, cytoskeleton, and  
343 the nucleus. Application of optimum concentrations of permeabilization agents (mild detergents  
344 or toxins) leads to washout of cytosolic marker enzymes—such as lactate dehydrogenase—and  
345 results in the complete loss of cell viability, tested by nuclear staining using membrane-  
346 impermeable dyes, while mitochondrial function remains intact. Respiration of isolated  
347 mitochondria remains unaltered after the addition of low concentrations of digitonin or saponin.  
348 In addition to mechanical cell disruption during homogenization of tissue, permeabilization  
349 agents may be applied to ensure permeabilization of all cells. Suspensions of cells  
350 permeabilized in the respiration chamber and crude tissue homogenates contain all components  
351 of the cell at highly dilute concentrations. All mitochondria are retained in chemically-  
352 permeabilized mitochondrial preparations and crude tissue homogenates. In the preparation of  
353 isolated mitochondria, the cells or tissues are homogenized, and the mitochondria are separated  
354 from other cell fractions and purified by differential centrifugation, entailing the loss of a  
355 fraction of the total mitochondrial content. Typical mitochondrial recovery ranges from 30% to  
356 80%. Maximization of the purity of isolated mitochondria may compromise not only the  
357 mitochondrial yield but also the structural and functional integrity. Therefore, protocols to  
358 isolate mitochondria need to be optimized according to each study. The term mitochondrial  
359 preparation does not include further fractionation of mitochondrial components, neither  
360 submitochondrial particles.

361

### 362 *2.1. Respiratory control and coupling*

363

364 Respiratory coupling control states are established in studies of mitochondrial  
365 preparations to obtain reference values for various output variables. Physiological conditions *in*  
366 *vivo* deviate from these experimentally obtained states. Since kinetically-saturating  
367 concentrations, *e.g.*, of ADP or oxygen (O<sub>2</sub>; dioxygen), may not apply to physiological  
368 intracellular conditions, relevant information is obtained in studies of kinetic responses to  
369 variations in [ADP] or [O<sub>2</sub>] in the range between kinetically-saturating concentrations and  
370 anoxia (Gnaiger 2001).

371 **The steady-state:** Mitochondria represent a thermodynamically open system in non-  
372 equilibrium states of biochemical energy transformation. State variables (protonmotive force;  
373 redox states) and metabolic *rates* (fluxes) are measured in defined mitochondrial respiratory  
374 *states*. Steady-states can be obtained only in open systems, in which changes by *internal*  
375 transformations, *e.g.*, O<sub>2</sub> consumption, are instantaneously compensated for by *external* fluxes,  
376 *e.g.*, O<sub>2</sub> supply, preventing a change of O<sub>2</sub> concentration in the system (Gnaiger 1993b).  
377 Mitochondrial respiratory states monitored in closed systems satisfy the criteria of pseudo-  
378 steady states for limited periods of time, when changes in the system (concentrations of O<sub>2</sub>, fuel  
379 substrates, ADP, P<sub>i</sub>, H<sup>+</sup>) do not exert significant effects on metabolic fluxes (respiration,  
380 phosphorylation). Such pseudo-steady states require respiratory media with sufficient buffering  
381 capacity and substrates maintained at kinetically-saturating concentrations, and thus depend on  
382 the kinetics of the processes under investigation.

383 **Specification of biochemical dose:** Substrates, uncouplers, inhibitors, and other  
384 chemical reagents are titrated to dissect mitochondrial function. Nominal concentrations of  
385 these substances are usually reported as initial amount of substance concentration [mol·L<sup>-1</sup>] in  
386 the incubation medium. When aiming at the measurement of kinetically saturated processes—



387 such as OXPHOS-capacities, the concentrations for substrates can be chosen according to the  
 388 apparent equilibrium constant,  $K_m'$ . In the case of hyperbolic kinetics, only 80% of maximum  
 389 respiratory capacity is obtained at a substrate concentration of four times the  $K_m'$ , whereas  
 390 substrate concentrations of 5, 9, 19 and 49 times the  $K_m'$  are theoretically required for reaching  
 391 83%, 90%, 95% or 98% of the maximal rate (Gnaiger 2001). Other reagents are chosen to  
 392 inhibit or alter some processes. The amount of these chemicals in an experimental incubation  
 393 is selected to maximize effect, avoiding unacceptable off-target consequences that would  
 394 adversely affect the data being sought. Specifying the amount of substance in an incubation as  
 395 nominal concentration in the aqueous incubation medium can be ambiguous (Doskey *et al.*  
 396 2015), particularly for lipophilic substances (oligomycin, uncouplers, permeabilization agents)  
 397 or cations (TPP<sup>+</sup>; fluorescent dyes such as safranin, TMRM), which accumulate in biological  
 398 membranes or in the mitochondrial matrix. For example, a dose of digitonin of 8 fmol·cell<sup>-1</sup> (10  
 399 pg·cell<sup>-1</sup>; 10 µg·10<sup>-6</sup> cells) is optimal for permeabilization of endothelial cells, and the  
 400 concentration in the incubation medium has to be adjusted according to the cell density applied  
 401 (Doerrier *et al.* 2018).

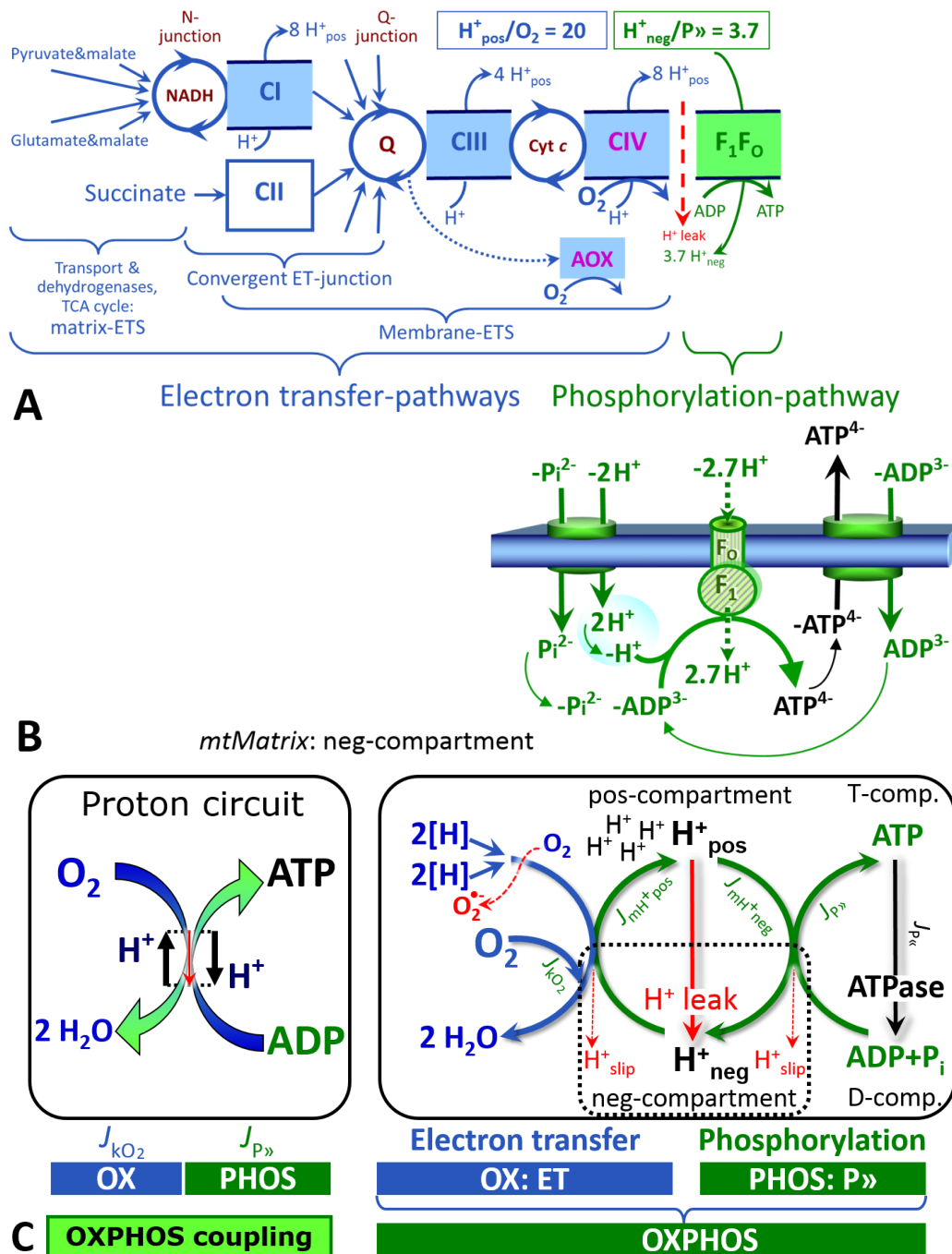
402 Generally, dose/exposure can be specified per unit of biological sample, *i.e.*, (nominal  
 403 moles of xenobiotic)/(number of cells) [mol·cell<sup>-1</sup>] or, as appropriate, per mass of biological  
 404 sample [mol·kg<sup>-1</sup>]. This approach to specification of dose/exposure provides a scalable  
 405 parameter that can be used to design experiments, help interpret a wide variety of experimental  
 406 results, and provide absolute information that allows researchers worldwide to make the most  
 407 use of published data (Doskey *et al.* 2015).

408 **Phosphorylation, P», and P»/O<sub>2</sub> ratio:** *Phosphorylation* in the context of OXPHOS is  
 409 defined as phosphorylation of ADP by P<sub>i</sub> to form ATP. On the other hand, the term  
 410 phosphorylation is used generally in many contexts, *e.g.*, protein phosphorylation. This justifies  
 411 consideration of a symbol more discriminating and specific than P as used in the P/O ratio  
 412 (phosphate to atomic oxygen ratio), where P indicates phosphorylation of ADP to ATP or GDP  
 413 to GTP (**Figure 1**). We propose the symbol P» for the endergonic (uphill) direction of  
 414 phosphorylation ADP→ATP, and likewise the symbol P« for the corresponding exergonic  
 415 (downhill) hydrolysis ATP→ADP (**Figure 2**). P» refers mainly to electrontransfer  
 416 phosphorylation but may also involve substrate-level phosphorylation as part of the  
 417 tricarboxylic acid (TCA) cycle (succinyl-CoA ligase; phosphoglycerate kinase) and  
 418 phosphorylation of ADP catalyzed by pyruvate kinase, and of GDP phosphorylated by  
 419 phosphoenolpyruvate carboxykinase. Transphosphorylation is performed by adenylate kinase,  
 420 creatine kinase, hexokinase and nucleoside diphosphate kinase. In isolated mammalian  
 421 mitochondria, ATP production catalyzed by adenylate kinase (2 ADP ↔ ATP + AMP) proceeds  
 422 without fuel substrates in the presence of ADP (Komlódi and Tretter 2017). Kinase cycles are  
 423 involved in intracellular energy transfer and signal transduction for regulation of energy flux.

424 The P»/O<sub>2</sub> ratio (P»/4 e<sup>-</sup>) is two times the 'P/O' ratio (P»/2 e<sup>-</sup>) of classical bioenergetics.  
 425 P»/O<sub>2</sub> is a generalized symbol, not specific for determination of P<sub>i</sub> consumption (P<sub>i</sub>/O<sub>2</sub> flux  
 426 ratio), ADP depletion (ADP/O<sub>2</sub> flux ratio), or ATP production (ATP/O<sub>2</sub> flux ratio). The  
 427 mechanistic P»/O<sub>2</sub> ratio—or P»/O<sub>2</sub> stoichiometry—is calculated from the proton-to-O<sub>2</sub> and  
 428 proton-to-phosphorylation coupling stoichiometries (**Figure 2A**):

$$429 \quad P»/O_2 = \frac{H_{\text{pos}/O_2}^+}{H_{\text{neg}/P»}^+} \quad (1)$$

430 The H<sup>+</sup><sub>pos</sub>/O<sub>2</sub> *coupling stoichiometry* (referring to the full 4 electron reduction of O<sub>2</sub>) depends  
 431 on the ET-pathway control state which defines the relative involvement of the three coupling  
 432 sites (CI, CIII and CIV) in the catabolic pathway of electrons to O<sub>2</sub>. This varies with: (1) a  
 433 bypass of CI by single or multiple electron input into the Q-junction; and (2) a bypass of CIV  
 434 by involvement of alternative oxidases, AOX, which are not expressed in mammalian  
 435 mitochondria.



436  
437  
438  
439  
440  
441  
442  
443  
444  
445  
446  
447  
448  
449

### Figure 2. Oxidative phosphorylation (OXPHOS).

(A) The mitochondrial electron transfer system (ETS) is fuelled by diffusion and transport of substrates across the mitochondrial outer and inner membrane and consists of the matrix-ETS and membrane-ETS. ET-pathways are coupled to the phosphorylation-pathway. ET-pathways converge at the N-junction and Q-junction. Additional arrows indicate electron entry into the Q-junction through electron transferring flavoprotein, glycerophosphate dehydrogenase, dihydro-ototate dehydrogenase, choline dehydrogenase, and sulfide-ubiquinone oxidoreductase. The dotted arrow indicates the branched pathway of oxygen consumption by alternative quinol oxidase (AOX). The  $H^+_{pos}/O_2$  ratio is the outward proton flux from the matrix space to the positively (pos) charged compartment, divided by catabolic  $O_2$  flux in the NADH-pathway. The  $H^+_{neg}/P$  ratio is the inward proton flux from the inter-membrane space to the negatively (neg) charged matrix space, divided by the flux of phosphorylation of ADP to ATP. These are not fixed stoichiometries due to ion leaks and proton slip.

450 (B) Phosphorylation-pathway catalyzed by the proton pump  $F_1F_0$ -ATPase (F-ATPase, ATP  
 451 synthase), adenine nucleotide translocase, and inorganic phosphate transporter. The  $H^+_{neg}/P_{\gg}$   
 452 stoichiometry is the sum of the coupling stoichiometry in the F-ATPase reaction ( $-2.7 H^+_{pos}$   
 453 from the positive intermembrane space,  $2.7 H^+$  to the matrix, *i.e.*, the negative compartment)  
 454 and the proton balance in the translocation of  $ADP^{2-}$ ,  $ATP^{3-}$  and  $P_i^{2-}$ .

455 (C) The proton circuit and coupling in OXPHOS.  $2[H]$  indicates the reduced hydrogen  
 456 equivalents of fuel substrates of the catabolic reaction  $k$  with oxygen.  $O_2$  flux,  $J_{kO_2}$ , through the  
 457 catabolic ET-pathway, is coupled to flux through the phosphorylation-pathway of ADP to ATP,  
 458  $J_{P_{\gg}}$ . The redox proton pumps of the ET-pathway drive proton flux into the positive (pos)  
 459 compartment,  $J_{mH^+pos}$ , generating the output protonmotive force (motive, subscript m). F-  
 460 ATPase is coupled to inward proton current into the negative (neg) compartment,  $J_{mH^+neg}$ , to  
 461 phosphorylate  $ADP+P_i$  to ATP. The system is defined by the boundaries (full black line) and is  
 462 not a black box, but is analysed as a compartmental system. The negative compartment (neg-  
 463 compartment, enclosed by the dotted line) is the matrix space, separated by the mtIM from the  
 464 positive compartment (pos-compartment).  $ADP+P_i$  and ATP are the substrate- and product-  
 465 compartments (scalar ADP and ATP compartments, D-comp. and T-comp.), respectively. At  
 466 steady-state proton turnover,  $J_{\infty H^+}$ , and ATP turnover,  $J_{\infty P}$ , maintain concentrations constant,  
 467 when  $J_{mH^+\infty} = J_{mH^+pos} = J_{mH^+neg}$ , and  $J_{P\infty} = J_{P_{\gg}} = J_{P_{\ll}}$ . Modified from (A) Lemieux *et al.* (2017)  
 468 and (B,C) Gnaiger (2014).

469  
 470  $H^+_{pos}/O_2$  is 12 in the ET-pathways involving CIII and CIV as proton pumps, increasing to  
 471 20 for the NADH-pathway (Figure 2A), but a general consensus on  $H^+_{pos}/O_2$  stoichiometries  
 472 remains to be reached (Hinkle 2005; Wikström and Hummer 2012; Sazanov 2015). The  
 473  $H^+_{neg}/P_{\gg}$  coupling stoichiometry (3.7; Figure 2A) is the sum of  $2.7 H^+_{neg}$  required by the F-  
 474 ATPase of vertebrate and most invertebrate species (Watt *et al.* 2010) and the proton balance  
 475 in the translocation of ADP, ATP and  $P_i$  (Figure 2B). Taken together, the mechanistic  $P_{\gg}/O_2$   
 476 ratio is calculated at 5.4 and 3.3 for NADH- and succinate-linked respiration, respectively (Eq.  
 477 1). The corresponding classical  $P_{\gg}/O$  ratios (referring to the 2 electron reduction of  $0.5 O_2$ ) are  
 478 2.7 and 1.6 (Watt *et al.* 2010), in agreement with the measured  $P_{\gg}/O$  ratio for succinate of  $1.58$   
 479  $\pm 0.02$  (Gnaiger *et al.* 2000).

480 The effective  $P_{\gg}/O_2$  flux ratio ( $Y_{P_{\gg}/O_2} = J_{P_{\gg}}/J_{kO_2}$ ) is diminished relative to the mechanistic  
 481  $P_{\gg}/O_2$  ratio by intrinsic and extrinsic uncoupling and dyscoupling (Figure 3). Such generalized  
 482 uncoupling is different from switching to mitochondrial pathways that involve fewer than three  
 483 proton pumps ('coupling sites': Complexes CI, CIII and CIV), bypassing CI through multiple  
 484 electron entries into the Q-junction, or CIII and CIV through AOX (Figure 2). Reprogramming  
 485 of mitochondrial pathways may be considered as a switch of gears (changing the stoichiometry)  
 486 rather than uncoupling (loosening the stoichiometry). In addition,  $Y_{P_{\gg}/O_2}$  depends on several  
 487 experimental conditions of flux control, increasing as a hyperbolic function of [ADP] to a  
 488 maximum value (Gnaiger 2001).

489 **Control and regulation:** The terms metabolic *control* and *regulation* are frequently used  
 490 synonymously, but are distinguished in metabolic control analysis: 'We could understand the  
 491 regulation as the mechanism that occurs when a system maintains some variable constant over  
 492 time, in spite of fluctuations in external conditions (homeostasis of the internal state). On the  
 493 other hand, metabolic control is the power to change the state of the metabolism in response to  
 494 an external signal' (Fell 1997). Respiratory control may be induced by experimental control  
 495 signals that *exert* an influence on: (1) ATP demand and ADP phosphorylation-rate; (2) fuel  
 496 substrate composition, pathway competition; (3) available amounts of substrates and  $O_2$ , *e.g.*,  
 497 starvation and hypoxia; (4) the protonmotive force, redox states, flux-force relationships,  
 498 coupling and efficiency; (5)  $Ca^{2+}$  and other ions including  $H^+$ ; (6) inhibitors, *e.g.*, nitric oxide  
 499 or intermediary metabolites such as oxaloacetate; (7) signalling pathways and regulatory  
 500 proteins, *e.g.*, insulin resistance, transcription factor hypoxia inducible factor 1. *Mechanisms of*

501 respiratory control and regulation include adjustments of: (1) enzyme activities by allosteric  
 502 mechanisms and phosphorylation; (2) enzyme content, concentrations of cofactors and  
 503 conserved moieties—such as adenylates, nicotinamide adenine dinucleotide [NAD<sup>+</sup>/NADH],  
 504 coenzyme Q, cytochrome *c*; (3) metabolic channeling by supercomplexes; and (4)  
 505 mitochondrial density (enzyme concentrations and membrane area) and morphology (cristae  
 506 folding, fission and fusion). Mitochondria are targeted directly by hormones, thereby affecting  
 507 their energy metabolism (Lee *et al.* 2013; Gerö and Szabo 2016; Price and Dai 2016; Moreno  
 508 *et al.* 2017). Evolutionary or acquired differences in the genetic and epigenetic basis of  
 509 mitochondrial function (or dysfunction) between subjects and gene therapy; age; gender,  
 510 biological sex, and hormone concentrations; life style including exercise and nutrition; and  
 511 environmental issues including thermal, atmospheric, toxicological and pharmacological  
 512 factors, exert an influence on all control mechanisms listed above. For reviews, see Brown  
 513 1992; Gnaiger 1993a, 2009; 2014; Paradies *et al.* 2014; Morrow *et al.* 2017.

514 **Respiratory control and response:** Lack of control by a metabolic pathway, *e.g.*,  
 515 phosphorylation-pathway, means that there will be no response to a variable activating it, *e.g.*,  
 516 [ADP]. The reverse, however, is not true as the absence of a response to [ADP] does not exclude  
 517 the phosphorylation-pathway from having some degree of control. The degree of control of a  
 518 component of the OXPHOS-pathway on an output variable—such as O<sub>2</sub> flux, will in general  
 519 be different from the degree of control on other outputs—such as phosphorylation-flux or  
 520 proton leak flux. Therefore, it is necessary to be specific as to which input and output are under  
 521 consideration (Fell 1997).

522 **Respiratory coupling control and ET-pathway control:** Respiratory control refers to  
 523 the ability of mitochondria to adjust O<sub>2</sub> flux in response to external control signals by engaging  
 524 various mechanisms of control and regulation. Respiratory control is monitored in a  
 525 mitochondrial preparation under conditions defined as respiratory states. When  
 526 phosphorylation of ADP to ATP is stimulated or depressed, an increase or decrease is observed  
 527 in electron transfer measured as O<sub>2</sub> flux in respiratory coupling states of intact mitochondria  
 528 (‘controlled states’ in the classical terminology of bioenergetics). Alternatively, coupling of  
 529 electron transfer with phosphorylation is disengaged by uncouplers. These protonophores are  
 530 weak lipid-soluble acids which disrupt the barrier function of the mtIM and thus shortcircuit  
 531 the protonmotive system, functioning like a clutch in a mechanical system. The corresponding  
 532 coupling control state is characterized by a high O<sub>2</sub> flux without control by P<sub>o</sub> (‘uncontrolled  
 533 state’).

534 ET-pathway control states are obtained in mitochondrial preparations by depletion of  
 535 endogenous substrates and addition to the mitochondrial respiration medium of fuel substrates  
 536 (2[H] in **Figure 2C**) and specific inhibitors, activating selected mitochondrial catabolic  
 537 pathways, *k* (**Figure 2A**). Coupling control states and pathway control states are  
 538 complementary, since mitochondrial preparations depend on an exogenous supply of pathway-  
 539 specific fuel substrates and oxygen (Gnaiger 2014).

540 **Coupling:** In mitochondrial electron transfer, vectorial transmembrane proton flux is  
 541 coupled through the redox proton pumps CI, CIII and CIV to the catabolic flux of scalar  
 542 reactions, collectively measured as O<sub>2</sub> flux (**Figure 2**). Thus mitochondria are elements of  
 543 energy transformation. Energy cannot be lost or produced in any internal process (First Law of  
 544 thermodynamics). Open and closed systems can gain or lose energy only by external fluxes—  
 545 by exchange with the environment. Energy is a conserved quantity. Therefore, energy can  
 546 neither be produced by mitochondria, nor is there any internal process without energy  
 547 conservation. Exergy is defined as the ‘free energy’ with the potential to perform work.  
 548 *Coupling* is the mechanistic linkage of an exergonic process (spontaneous, negative exergy  
 549 change) with an endergonic process (positive exergy change) in energy transformations which  
 550 conserve part of the exergy that would be irreversibly lost or dissipated in an uncoupled process.

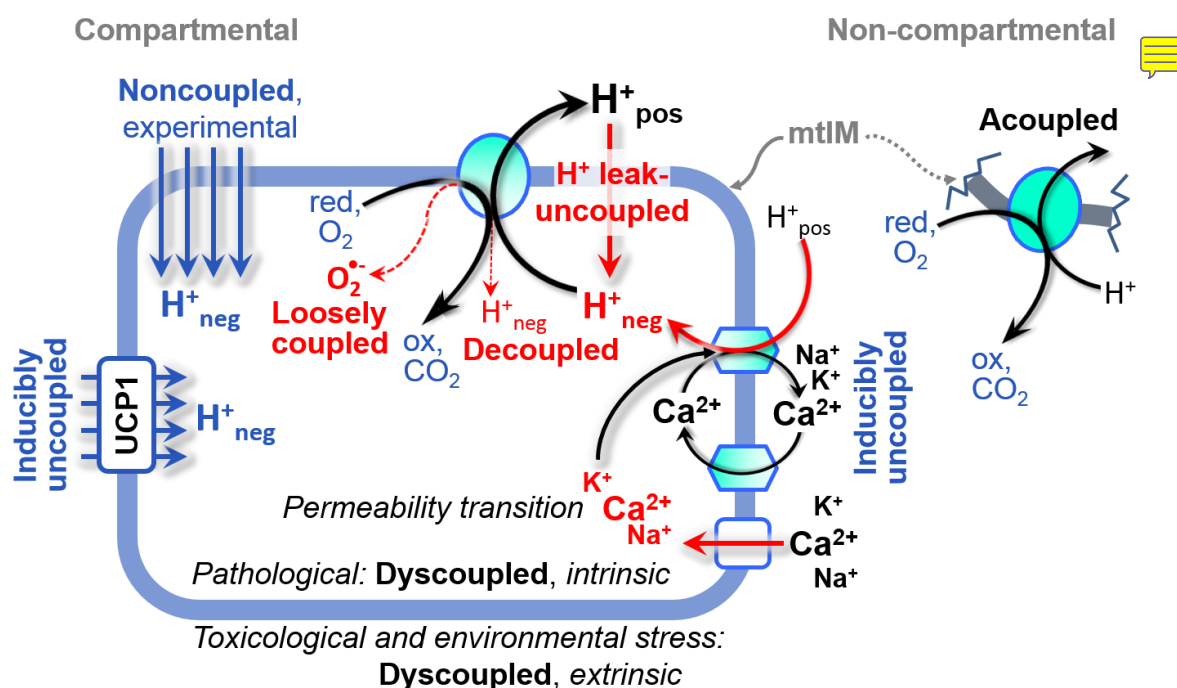


551 **Uncoupling:** Uncoupling of mitochondrial respiration is a general term comprising  
 552 diverse mechanisms:

- 553 1. Proton leak across the mtIM from the pos- to the neg-compartment (**Figure 2C**);
- 554 2. Cycling of other cations, strongly stimulated by permeability transition, or  
 555 experimentally induced by valinomycin in the presence of  $K^+$ ;
- 556 3. Proton slip in the redox proton pumps when protons are effectively not pumped (CI,  
 557 CIII and CIV) or are not driving phosphorylation (F-ATPase);
- 558 4. Loss of compartmental integrity when electron transfer is uncoupled;
- 559 5. Electron leak in the loosely coupled univalent reduction of  $O_2$  to superoxide ( $O_2^{\cdot-}$ ;  
 560 superoxide anion radical).

561 Differences of terms—uncoupled vs. noncoupled—are easily overlooked, although they relate  
 562 to different meanings of uncoupling (**Figure 3**).

563



564

### 565 **Figure 3. Mechanisms of respiratory uncoupling**

566 An intact mitochondrial inner membrane, mtIM, is required for vectorial, compartmental  
 567 coupling. ‘Acoupled’ respiration is the consequence of structural disruption with catalytic  
 568 activity of non-compartmental mitochondrial fragments. Inducibly uncoupled (activation of  
 569 UCP1) and experimentally noncoupled respiration (titration of protonophores) stimulate  
 570 respiration to maximum  $O_2$  flux.  $H^+$  leak-uncoupled, decoupled, and loosely coupled respiration  
 571 are components of intrinsic uncoupling. Pathological dysfunction may affect all types of  
 572 uncoupling, including permeability transition, causing intrinsically dyscoupled respiration.  
 573 Similarly, toxicological and environmental stress factors can cause extrinsically dyscoupled  
 574 respiration.

575

### 576 **2.2. Coupling states and respiratory rates**

577

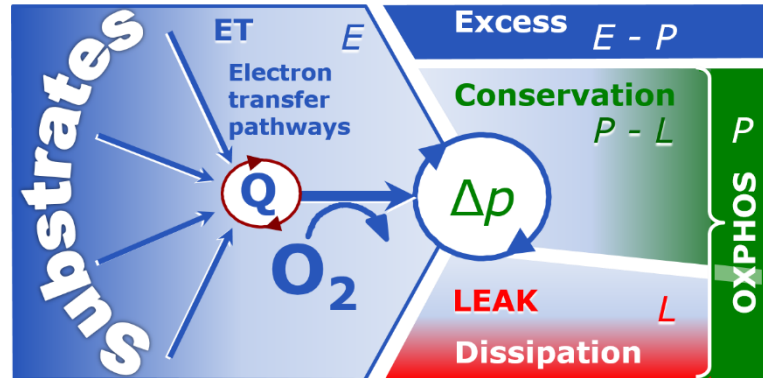
578 **Respiratory capacities in coupling control states:** To extend the classical nomenclature  
 579 on mitochondrial coupling states (Section 2.3) by a concept-driven terminology that  
 580 incorporates explicitly information on the meaning of respiratory states, the terminology must  
 581 be general and not restricted to any particular experimental protocol or mitochondrial  
 582 preparation (Gnaiger 2009). Concept-driven nomenclature aims at mapping the *meaning and*  
 583 *concept behind* the words and acronyms onto the *forms* of words and acronyms (Miller 1991).



584 The focus of concept-driven nomenclature is primarily the conceptual ‘why’, along with  
 585 clarification of the experimental ‘how’. Respiratory capacities delineate, comparable to channel  
 586 capacity in information theory (Schneider 2006), the upper bound of the rate of respiration  
 587 measured in defined coupling control states and electron transfer-pathway (ET-pathway) states  
 588 (Figure 4).

590 **Figure 4. Four-compartment model of oxidative phosphorylation**

591 Respiratory states (ET, OXPHOS, LEAK; Table 1) and corresponding rates ( $E$ ,  $P$ ,  $L$ ) are  
 592 connected by the protonmotive force,  $\Delta p$ . ET-capacity,  $E$ , is  
 593 partitioned into (1) dissipative LEAK-respiration,  $L$ , when the  
 594 Gibbs energy change of catabolic



595  $O_2$  flux is irreversibly lost, (2) net OXPHOS-capacity,  $P-L$ , with partial conservation of the  
 596 capacity to perform work, and (3) the excess capacity,  $E-P$ . Modified from Gnaiger (2014).

603

604 **Table 1. Coupling states and residual oxygen consumption in mitochondrial preparations in relation to respiration- and phosphorylation-flux,  $J_{kO_2}$  and  $J_{P_{\gg}}$ , and protonmotive force,  $\Delta p$ .** Coupling states are established at kinetically-saturating concentrations of fuel substrates and  $O_2$ .

State	$J_{kO_2}$	$J_{P_{\gg}}$	$\Delta p$	Inducing factors	Limiting factors
LEAK	$L$ ; low, cation leak-dependent respiration	0	max.	proton leak, slip, and cation cycling	$J_{P_{\gg}} = 0$ : (1) without ADP, $L_N$ ; (2) max. ATP/ADP ratio, $L_T$ ; or (3) inhibition of the phosphorylation-pathway, $L_{Omy}$
OXPHOS	$P$ ; high, ADP-stimulated respiration	max.	high	kinetically-saturating [ADP] and $[P_i]$	$J_{P_{\gg}}$ by phosphorylation-pathway; or $J_{kO_2}$ by ET-capacity
ET	$E$ ; max., noncoupled respiration	0	low	optimal external uncoupler concentration for max. $J_{O_2, E}$	$J_{kO_2}$ by ET-capacity
ROX	$R_{ox}$ ; min., residual $O_2$ consumption	0	0	$J_{O_2, Rox}$ in non-ET-pathway oxidation reactions	full inhibition of ET-pathway; or absence of fuel substrates

608

609 To provide a diagnostic reference for respiratory capacities of core energy metabolism,  
 610 the capacity of *oxidative phosphorylation*, OXPHOS, is measured at kinetically-saturating  
 611 concentrations of ADP and  $P_i$ . The *oxidative* ET-capacity reveals the limitation of OXPHOS-  
 612 capacity mediated by the *phosphorylation*-pathway. The ET- and phosphorylation-pathways  
 613 comprise coupled segments of the OXPHOS-system. ET-capacity is measured as noncoupled  
 614 respiration by application of *external uncouplers*. The contribution of *intrinsically uncoupled*

615 O<sub>2</sub> consumption is studied by preventing the stimulation of phosphorylation either in the  
 616 absence of ADP or by inhibition of the phosphorylation-pathway. The corresponding states are  
 617 collectively classified as LEAK-states, when O<sub>2</sub> consumption compensates mainly for ion  
 618 leaks, including the proton leak. Defined coupling states are induced by: (1) adding cation  
 619 chelators such as EGTA, binding free Ca<sup>2+</sup> and thus limiting cation cycling; (2) adding ADP  
 620 and P<sub>i</sub>; (3) inhibiting the phosphorylation-pathway; and (4) uncoupler titrations, while  
 621 maintaining a defined ET-pathway state with constant fuel substrates and inhibitors of specific  
 622 branches of the ET-pathway (**Figure 4**).

623  
 624 The three coupling states,  
 625 ET, LEAK and OXPHOS, are  
 626 shown schematically with the  
 627 corresponding respiratory rates,  
 628 abbreviated as *E*, *L* and *P*,  
 629 respectively (**Figure 4**). We  
 630 distinguish metabolic *pathways*  
 631 from metabolic *states* and the  
 632 corresponding metabolic *rates*;  
 633 for example: ET-pathways  
 634 (**Figure 4**), ET-states (**Figure**  
 635 **5C**), and ET-capacities, *E*,  
 636 respectively (**Table 1**). The  
 637 protonmotive force is *high* in the  
 638 OXPHOS-state when it drives  
 639 phosphorylation, *maximum* in the  
 640 LEAK-state of coupled  
 641 mitochondria, driven by LEAK-  
 642 respiration at a minimum back  
 643 flux of cations to the matrix side,  
 644 and *very low* in the ET-state  
 645 when uncouplers short-circuit the  
 646 proton cycle (**Table 1**).

647 **LEAK-state (Figure 5A):**  
 648 The LEAK-state is defined as a  
 649 state of mitochondrial respiration  
 650 when O<sub>2</sub> flux mainly  
 651 compensates for ion leaks in the  
 652 absence of ATP synthesis, at  
 653 kinetically-saturating  
 654 concentrations of O<sub>2</sub> and  
 655 respiratory fuel substrates.  
 656 LEAK-respiration is measured to  
 657 obtain an estimate of *intrinsic*  
 658 *uncoupling* without addition of  
 659 an experimental uncoupler: (1)  
 660 in the absence of adenylates, *i.e.*,  
 661 AMP, ADP and ATP; (2) after  
 662 depletion of ADP at a maximum  
 663 ATP/ADP ratio; or (3) after  
 664 inhibition of the  
 665 phosphorylation-pathway by

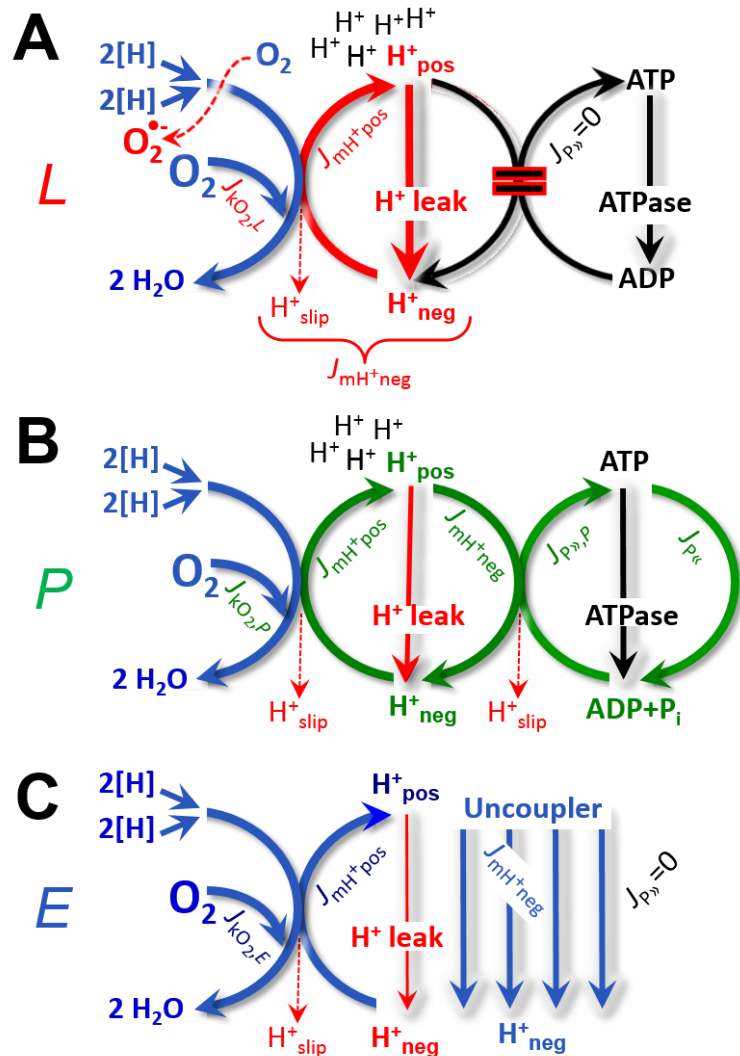


**Figure 5. Respiratory coupling states**

(A) **LEAK-state and rate, *L***: Phosphorylation is arrested,  $J_{P_{\gg}} = 0$ , and catabolic O<sub>2</sub> flux,  $J_{kO_2,L}$ , is controlled mainly by the proton leak,  $J_{mH^{+}neg,L}$ , at maximum protonmotive force (**Figure 3**).

(B) **OXPHOS-state and rate, *P***: Phosphorylation,  $J_{P_{\gg}}$ , is stimulated by kinetically-saturating [ADP] and [P<sub>i</sub>], and is supported by a high protonmotive force. O<sub>2</sub> flux,  $J_{kO_2,P}$ , is well-coupled at a  $P_{\gg}/O_2$  ratio of  $J_{P_{\gg},P}/J_{O_2,P}$ .

(C) **ET-state and rate, *E***: Noncoupled respiration,  $J_{kO_2,E}$ , is maximum at optimum exogenous uncoupler concentration and phosphorylation is zero,  $J_{P_{\gg}} = 0$ . See also **Figure 2**.

666 inhibitors of F-ATPase—such as oligomycin, or of adenine nucleotide translocase—such as  
 667 carboxyatractyloside. Adjustment of the nominal concentration of these inhibitors to the density  
 668 of biological sample applied can minimize or avoid inhibitory side-effects exerted on ET-  
 669 capacity or even some dyscoupling.

670 **Proton leak and uncoupled respiration:** Proton leak is a leak current of protons. The  
 671 intrinsic proton leak is the *uncoupled* process in which protons diffuse across the mtIM in the  
 672 dissipative direction of the downhill protonmotive force without coupling to phosphorylation  
 673 (**Figure 5A**). The proton leak flux depends non-linearly on the protonmotive force (Garlid *et*  
 674 *al.* 1989; Divakaruni and Brand 2011), it is a property of the mtIM and may be enhanced due  
 675 to possible contaminations by free fatty acids. Inducible uncoupling mediated by uncoupling  
 676 protein 1 (UCP1) is physiologically controlled, *e.g.*, in brown adipose tissue. UCP1 is a member  
 677 of the mitochondrial carrier family which is involved in the translocation of protons across the  
 678 mtIM (Klingenberg 2017). Consequently, the short-circuit diminishes the protonmotive force  
 679 and stimulates electron transfer to O<sub>2</sub> and heat dissipation without phosphorylation of ADP.

680 **Cation cycling:** There can be other cation contributors to leak current including calcium  
 681 and probably magnesium. Calcium current is balanced by mitochondrial Na<sup>+</sup>/Ca<sup>2+</sup> exchange,  
 682 which is balanced by Na<sup>+</sup>/H<sup>+</sup> or K<sup>+</sup>/H<sup>+</sup> exchanges. This is another effective uncoupling  
 683 mechanism different from proton leak (**Table 2**).

684 **Table 2. Terms on respiratory coupling and uncoupling.**  
 685

Term	$J_{\text{K}O_2}$	$P \gg O_2$	Note	
acoupled		0	electron transfer in mitochondrial fragments without vectorial proton translocation ( <b>Figure 3</b> )	
intrinsic, no protonophore added	uncoupled	$L$	0	non-phosphorylating LEAK-respiration ( <b>Figure 5A</b> )
	proton leak-uncoupled		0	component of $L$ , H <sup>+</sup> diffusion across the mtIM ( <b>Figure 3</b> )
	decoupled		0	component of $L$ , proton slip ( <b>Figure 3</b> )
	loosely coupled		0	component of $L$ , lower coupling due to superoxide formation and bypass of proton pumps ( <b>Figure 3</b> )
	dyscoupled		0	pathologically, toxicologically, environmentally increased uncoupling, mitochondrial dysfunction
	inducibly uncoupled		0	by UCP1 or cation ( <i>e.g.</i> , Ca <sup>2+</sup> ) cycling ( <b>Figure 3</b> )
noncoupled	$E$	0	non-phosphorylating respiration stimulated to maximum flux at optimum exogenous uncoupler concentration ( <b>Figure 5C</b> )	
well-coupled	$P$	high	phosphorylating respiration with an intrinsic LEAK component ( <b>Figure 5B</b> )	
fully coupled	$P - L$	max.	OXPPOS-capacity corrected for LEAK-respiration ( <b>Figure 4</b> )	

686 **Proton slip and decoupled respiration:** Proton slip is the *decoupled* process in which  
 687 protons are only partially translocated by a redox proton pump of the ET-pathways and slip  
 688 back to the original compartment. The proton leak is the dominant contributor to the overall  
 689 leak current in mammalian mitochondria incubated under physiological conditions at 37 °C,  
 690 whereas proton slip is increased at lower experimental temperature (Canton *et al.* 1995). Proton  
 691

692 slip can also happen in association with the F-ATPase, in which the proton slips downhill across  
 693 the pump to the matrix without contributing to ATP synthesis. In each case, proton slip is a  
 694 property of the proton pump and increases with the pump turnover rate.

695 **Electron leak and loosely coupled respiration:** Superoxide production by the ETS leads  
 696 to a bypass of redox proton pumps and correspondingly lower  $P_{\gg}/O_2$  ratio. This depends on the  
 697 actual site of electron leak and the scavenging of hydrogen peroxide by cytochrome *c*, whereby  
 698 electrons may re-enter the ETS with proton translocation by CIV.

699 **Loss of compartmental integrity and acoupled respiration:** Electron transfer and  
 700 catabolic  $O_2$  flux proceed without compartmental proton translocation in disrupted  
 701 mitochondrial fragments. Such fragments form during mitochondrial isolation, and may not  
 702 fully fuse to re-establish structurally intact mitochondria. Loss of mtIM integrity, therefore, is  
 703 the cause of acoupled respiration, which is a nonvectorial dissipative process without control  
 704 by the protonmotive force.

705 **Dyscoupled respiration:** Mitochondrial injuries may lead to *dyscoupling* as a  
 706 pathological or toxicological cause of *uncoupled* respiration. Dyscoupling may involve any  
 707 type of uncoupling mechanism, *e.g.*, opening the permeability transition pore. Dyscoupled  
 708 respiration is distinguished from the experimentally induced *noncoupled* respiration in the ET-  
 709 state (**Table 2**).

710 **OXPPOS-state (Figure 5B):** The OXPPOS-state is defined as the respiratory state with  
 711 kinetically-saturating concentrations of  $O_2$ , respiratory and phosphorylation substrates, and  
 712 absence of exogenous uncoupler, which provides an estimate of the maximal respiratory  
 713 capacity in the OXPPOS-state for any given ET-pathway state. Respiratory capacities at  
 714 kinetically-saturating substrate concentrations provide reference values or upper limits of  
 715 performance, aiming at the generation of data sets for comparative purposes. Physiological  
 716 activities and effects of substrate kinetics can be evaluated relative to the OXPPOS-capacity.

717 As discussed previously, 0.2 mM ADP does not fully saturate flux in isolated  
 718 mitochondria (Gnaiger 2001; Puchowicz *et al.* 2004); greater ADP concentration is required,  
 719 particularly in permeabilized muscle fibres and cardiomyocytes, to overcome limitations by  
 720 intracellular diffusion and by the reduced conductance of the mtOM (Jepihhina *et al.* 2011,  
 721 Illaste *et al.* 2012, Simson *et al.* 2016), either through interaction with tubulin (Rostovtseva *et*  
 722 *al.* 2008) or other intracellular structures (Birkedal *et al.* 2014). In permeabilized muscle fibre  
 723 bundles of high respiratory capacity, the apparent  $K_m$  for ADP increases up to 0.5 mM (Saks *et*  
 724 *al.* 1998), consistent with experimental evidence that >90% saturation is reached only at >5  
 725 mM ADP (Pesta and Gnaiger 2012). Similar ADP concentrations are also required for accurate  
 726 determination of OXPPOS-capacity in human clinical cancer samples and permeabilized cells  
 727 (Klepinin *et al.* 2016; Koit *et al.* 2017). Whereas 2.5 to 5 mM ADP is sufficient to obtain the  
 728 actual OXPPOS-capacity in many types of permeabilized tissue and cell preparations,  
 729 experimental validation is required in each specific case.

730 **Electron transfer-state (Figure 5C):** The ET-state is defined as the *noncoupled* state  
 731 with kinetically-saturating concentrations of  $O_2$ , respiratory substrate and optimum *exogenous*  
 732 uncoupler concentration for maximum  $O_2$  flux.  $O_2$  flux determined in the ET-state yields an  
 733 estimate of ET-capacity. Inhibition of respiration is observed above optimum uncoupler  
 734 concentrations. As a consequence of the nearly collapsed protonmotive force, the driving force  
 735 is insufficient for phosphorylation, and  $J_{P_{\gg}} = 0$ .

736 **ROX state and Rox:** Besides the three fundamental coupling states of mitochondrial  
 737 preparations, the state of residual  $O_2$  consumption, ROX, is relevant to assess respiratory  
 738 function. ROX is not a coupling state. The rate of residual oxygen consumption, *Rox*, is defined  
 739 as  $O_2$  consumption due to oxidative reactions measured after inhibition of ET—with rotenone,  
 740 malonic acid and antimycin A. Cyanide and azide inhibit not only CIV but catalase and several  
 741 peroxidases involved in *Rox*. However, high concentrations of antimycin A, but not rotenone  
 742 or cyanide, inhibit peroxisomal acyl-CoA oxidase and D-amino acid oxidase (Vamecq *et al.*



1987). ROX represents a baseline that is used to correct respiration in defined coupling states. *Rox* is not necessarily equivalent to non-mitochondrial reduction of O<sub>2</sub>, considering O<sub>2</sub>-consuming reactions in mitochondria that are not related to ET—such as O<sub>2</sub> consumption in reactions catalyzed by monoamine oxidases (type A and B), monooxygenases (cytochrome P450 monooxygenases), dioxygenase (sulfur dioxygenase and trimethyllysine dioxygenase), and several hydroxylases. Even isolated mitochondrial fractions, especially those obtained from liver, may be contaminated by peroxisomes. This fact makes the exact determination of mitochondrial O<sub>2</sub> consumption and mitochondria-associated generation of reactive oxygen species complicated (Schönfeld *et al.* 2009; Speijer 2016; **Figure 1**). The dependence of ROX-linked O<sub>2</sub> consumption needs to be studied in detail together with non-ET enzyme activities, availability of specific substrates, O<sub>2</sub> concentration, and electron leakage leading to the formation of reactive oxygen species.

**Quantitative relations:** *E* may exceed or be equal to *P*.  $E > P$  is observed in many types of mitochondria, varying between species, tissues and cell types (Gnaiger 2009).  $E - P$  is the excess ET-capacity pushing the phosphorylation-flux (**Figure 2B**) to the limit of its *capacity of utilizing* the protonmotive force. In addition, the magnitude of  $E - P$  depends on the tightness of respiratory coupling or degree of uncoupling, since an increase of *L* causes *P* to increase towards the limit of *E*. The *excess E-P* capacity,  $E - P$ , therefore, provides a sensitive diagnostic indicator of specific injuries of the phosphorylation-pathway, under conditions when *E* remains constant but *P* declines relative to controls (**Figure 4**). Substrate cocktails supporting simultaneous convergent electron transfer to the Q-junction for reconstitution of TCA cycle function establish pathway control states with high ET-capacity, and consequently increase the sensitivity of the  $E - P$  assay.

*E* cannot theoretically be lower than *P*.  $E < P$  must be discounted as an artefact, which may be caused experimentally by: (1) loss of oxidative capacity during the time course of the respirometric assay, since *E* is measured subsequently to *P*; (2) using insufficient uncoupler concentrations; (3) using high uncoupler concentrations which inhibit ET (Gnaiger 2008); (4) high oligomycin concentrations applied for measurement of *L* before titrations of uncoupler, when oligomycin exerts an inhibitory effect on *E*. On the other hand, the excess ET-capacity is overestimated if non-saturating [ADP] or [P<sub>i</sub>] are used. See State 3 in the next section.

The net OXPHOS-capacity is calculated by subtracting *L* from *P* (**Figure 4**). Then the net P<sub>»</sub>/O<sub>2</sub> equals P<sub>»</sub>/(*P*-*L*), wherein the dissipative LEAK component in the OXPHOS-state may be overestimated. This can be avoided by measuring LEAK-respiration in a state when the protonmotive force is adjusted to its slightly lower value in the OXPHOS-state—by titration of an ET inhibitor (Divakaruni and Brand 2011). Any turnover-dependent components of proton leak and slip, however, are underestimated under these conditions (Garlid *et al.* 1993). In general, it is inappropriate to use the term *ATP production* or *ATP turnover* for the difference of O<sub>2</sub> flux measured in states *P* and *L*. The difference *P*-*L* is the upper limit of the part of OXPHOS-capacity that is freely available for ATP production (corrected for LEAK-respiration) and is fully coupled to phosphorylation with a maximum mechanistic stoichiometry (**Figure 4**).

784

### 785 2.3. Classical terminology for isolated mitochondria

786 ‘When a code is familiar enough, it ceases appearing like a code; one forgets that there  
787 is a decoding mechanism. The message is identical with its meaning’ (Hofstadter 1979).  
788

789 Chance and Williams (1955; 1956) introduced five classical states of mitochondrial  
790 respiration and cytochrome redox states. **Table 3** shows a protocol with isolated mitochondria  
791 in a closed respirometric chamber, defining a sequence of respiratory states. States and rates  
792 are not specifically distinguished in this nomenclature.  
793



794  
795  
796**Table 3. Metabolic states of mitochondria (Chance and Williams, 1956; Table V).**

State	[O <sub>2</sub> ]	ADP level	Substrate level	Respiration rate	Rate-limiting substance
1	>0	Low	low	slow	ADP
2	>0	high	~0	slow	substrate
3	>0	high	high	fast	respiratory chain
4	>0	Low	high	slow	ADP
5	0	high	high	0	oxygen

797

798

799

800

**State 1** is obtained after addition of isolated mitochondria to air-saturated isoosmotic/isotonic respiration medium containing P<sub>i</sub>, but no fuel substrates and no adenylates, *i.e.*, AMP, ADP, ATP.

801

802

803

804

805

806

807

808

809

810

811

812

**State 2** is induced by addition of a ‘high’ concentration of ADP (typically 100 to 300 μM), which stimulates respiration transiently on the basis of endogenous fuel substrates and phosphorylates only a small portion of the added ADP. State 2 is then obtained at a low respiratory activity limited by exhausted endogenous fuel substrate availability (**Table 3**). If addition of specific inhibitors of respiratory complexes—such as rotenone—does not cause a further decline of O<sub>2</sub> flux, State 2 is equivalent to the ROX state (See below.). If inhibition is observed, undefined endogenous fuel substrates are a confounding factor of pathway control, contributing to the effect of subsequently externally added substrates and inhibitors. In contrast to the original protocol, an alternative sequence of titration steps is frequently applied, in which the alternative ‘State 2’ has an entirely different meaning, when this second state is induced by addition of fuel substrate without ADP (LEAK-state; in contrast to State 2 defined in **Table 1** as a ROX state), followed by addition of ADP.

813

814

815

816

817

818

819

820

821

822

823

824

825

**State 3** is the state stimulated by addition of fuel substrates while the ADP concentration is still high (**Table 3**) and supports coupled energy transformation through oxidative phosphorylation. ‘High ADP’ is a concentration of ADP specifically selected to allow the measurement of State 3 to State 4 transitions of isolated mitochondria in a closed respirometric chamber. Repeated ADP titration re-establishes State 3 at ‘high ADP’. Starting at O<sub>2</sub> concentrations near air-saturation (ca. 200 μM O<sub>2</sub> at sea level and 37 °C), the total ADP concentration added must be low enough (typically 100 to 300 μM) to allow phosphorylation to ATP at a coupled O<sub>2</sub> flux that does not lead to O<sub>2</sub> depletion during the transition to State 4. In contrast, kinetically-saturating ADP concentrations usually are 10-fold higher than ‘high ADP’, *e.g.*, 2.5 mM in isolated mitochondria. The abbreviation State 3u is occasionally used in bioenergetics, to indicate the state of respiration after titration of an uncoupler, without sufficient emphasis on the fundamental difference between OXPHOS-capacity (*well-coupled* with an *endogenous* uncoupled component) and ET-capacity (*noncoupled*).

826

827

828

829

830

831

832

833

834

835

836

837

**State 4** is a LEAK-state that is obtained only if the mitochondrial preparation is intact and well-coupled. Depletion of ADP by phosphorylation to ATP causes a decline of O<sub>2</sub> flux in the transition from State 3 to State 4. Under the conditions of State 4, a maximum protonmotive force and high ATP/ADP ratio are maintained. The gradual decline of  $Y_{P_{i}/O_2}$  towards diminishing [ADP] at State 4 must be taken into account for calculation of P<sub>»</sub>/O<sub>2</sub> ratios (Gnaiger 2001). State 4 respiration, L<sub>T</sub> (**Table 1**), reflects intrinsic proton leak and ATP hydrolysis activity. O<sub>2</sub> flux in State 4 is an overestimation of LEAK-respiration if the contaminating ATP hydrolysis activity recycles some ATP to ADP, J<sub>P<sub>«</sub></sub>, which stimulates respiration coupled to phosphorylation, J<sub>P<sub>»</sub></sub> > 0. This can be tested by inhibition of the phosphorylation-pathway using oligomycin, ensuring that J<sub>P<sub>»</sub></sub> = 0 (State 4o). Alternatively, sequential ADP titrations re-establish State 3, followed by State 3 to State 4 transitions while sufficient O<sub>2</sub> is available. Anoxia may be reached, however, before exhaustion of ADP (State 5).

838 **State 5** is the state after exhaustion of  $O_2$  in a closed respirometric chamber. Diffusion of  
 839  $O_2$  from the surroundings into the aqueous solution may be a confounding factor preventing  
 840 complete anoxia (Gnaiger 2001). Chance and Williams (1955) provide an alternative definition  
 841 of State 5, which gives it the different meaning of ROX versus anoxia: ‘State 5 may be obtained  
 842 by antimycin A treatment or by anaerobiosis’.

843 In **Table 3**, only States 3 and 4 (and ‘State 2’ in the alternative protocol: addition of fuel  
 844 substrates without ADP; not included in the table) are coupling control states, with the  
 845 restriction that  $O_2$  flux in State 3 may be limited kinetically by non-saturating ADP  
 846 concentrations (**Table 1**).

847  
 848

### 849 3. Normalization: fluxes and flows

850

#### 851 3.1. Normalization: system or sample

852

853 The term *rate* is not sufficiently defined to be useful for reporting data (**Figure 6**). The  
 854 inconsistency of the meanings of rate becomes fully apparent when considering Galileo  
 855 Galilei’s famous principle, that ‘bodies of different weight all fall at the same rate (have a  
 856 constant acceleration)’ (Coopersmith 2010).

857

#### 858 **Figure 6. Flow and flux, with system- or sample-specific normalization**

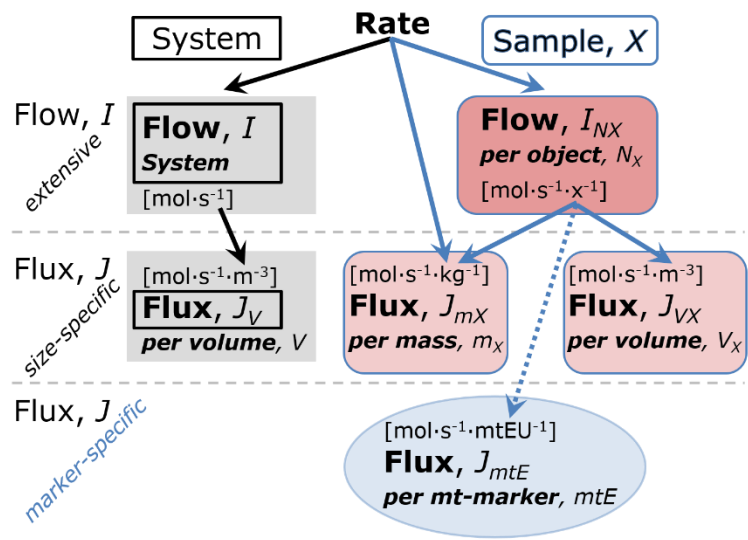
859 Different meanings of rate may lead to confusion, if the normalization is not sufficiently  
 860 specified. Results are frequently expressed as mass-specific *flux*,  
 861  $J_{mX}$ , per mg protein, dry or wet weight (mass). Cell volume,  $V_{\text{cell}}$ ,  
 862 may be used for normalization (volume-specific flux,  $J_{V\text{cell}}$ ),  
 863 which must be clearly distinguished from flow per cell,  
 864  $I_{N\text{cell}}$ , or flux,  $J_V$ , expressed for methodological reasons per volume of the measurement system. For details see **Table 4**.

874

875 **Flow per system,  $I$ :** In a generalization of electrical terms, flow as an extensive quantity  
 876 ( $I$ ; per system) is distinguished from flux as a size-specific quantity ( $J$ ; per system size) (**Figure**  
 877 **6**). Electric current is flow,  $I_{\text{el}}$  [ $A \equiv C \cdot s^{-1}$ ] per system (extensive quantity). When dividing this  
 878 extensive quantity by system size (cross-sectional area of a ‘wire’), a size-specific quantity is  
 879 obtained, which is flux (current density),  $J_{\text{el}}$  [ $A \cdot m^{-2} = C \cdot s^{-1} \cdot m^{-2}$ ].

880 **Extensive quantities:** An extensive quantity increases proportionally with system size.  
 881 The magnitude of an extensive quantity is completely additive for non-interacting  
 882 subsystems—such as mass or flow expressed per defined system. The magnitude of these  
 883 quantities depends on the extent or size of the system (Cohen *et al.* 2008).

884 **Size-specific quantities:** ‘The adjective *specific* before the name of an extensive quantity  
 885 is often used to mean *divided by mass*’ (Cohen *et al.* 2008). In this system-paradigm, mass-  
 886 specific flux is flow divided by mass of the *system* (the total mass of everything within the  
 887 measuring chamber or reactor). A mass-specific quantity is independent of the extent of non-  
 888 interacting homogenous subsystems. Tissue-specific quantities (related to the *sample* in  
 889 contrast to the *system*) are of fundamental interest in the field of comparative mitochondrial



890 physiology, where *specific* refers to the *type of the sample* rather than *mass of the system*. The  
 891 term *specific*, therefore, must be clarified; *sample-specific*, e.g., muscle mass-specific  
 892 normalization, is distinguished from *system-specific* quantities (mass or volume; **Figure 6**).  
 893

---

## 894 **Box 2: Metabolic fluxes and flows: vectorial and scalar**

895  
 896 Fluxes are *vectors*, if they have *spatial* geometric direction in addition to magnitude.  
 897 Electric charge per unit time is electric flow or current,  $I_{el} = dQ_{el} \cdot dt^{-1}$  [A]. When expressed per  
 898 unit cross-sectional area,  $A$  [ $m^2$ ], a vector flux is obtained, which is current density or surface-  
 899 density of flow) perpendicular to the direction of flux,  $\mathbf{J}_{el} = I_{el} \cdot A^{-1}$  [ $A \cdot m^{-2}$ ] (Cohen et al. 2008).  
 900 For all transformations *flows*,  $I_{tr}$ , are defined as extensive quantities. Vector and scalar *fluxes*  
 901 are obtained as  $\mathbf{J}_{tr} = I_{tr} \cdot A^{-1}$  [ $mol \cdot s^{-1} \cdot m^{-2}$ ] and  $J_{tr} = I_{tr} \cdot V^{-1}$  [ $mol \cdot s^{-1} \cdot m^{-3}$ ], expressing flux as an area-  
 902 specific vector or volume-specific vectorial or scalar quantity, respectively (Gnaiger 1993b).

903 We suggest to define: (1) *vectorial* fluxes, which are translocations as functions of  
 904 *gradients* with direction in geometric space in continuous systems; (2) *vectorial* fluxes, which  
 905 describe translocations in discontinuous systems and are restricted to information on  
 906 *compartmental differences* (**Figure 2C**, transmembrane proton flux); and (3) *scalar* fluxes,  
 907 which are transformations in a *homogenous* system (**Figure 2C**, catabolic  $O_2$  flux,  $J_{kO_2}$ ).

908 Vectorial transmembrane proton fluxes,  $J_{mH^+pos}$  and  $J_{mH^+neg}$ , are analyzed in a  
 909 heterogenous compartmental system as a quantity with *directional* but not *spatial* information.  
 910 Translocation of protons across the mtIM has a defined direction, either from the negative  
 911 compartment (matrix space; negative, neg-compartment) to the positive compartment (inter-  
 912 membrane space; positive, pos-compartment) or *vice versa* (**Figure 2C**). The arrows defining  
 913 the direction of the translocation between the two compartments may point upwards or  
 914 downwards, right or left, without any implication that these are actual directions in space. The  
 915 pos-compartment is neither above nor below the neg-compartment in a spatial sense, but can  
 916 be visualized arbitrarily in a figure in the upper position (**Figure 2C**). In general, the  
 917 *compartmental direction* of vectorial translocation from the neg-compartment to the pos-  
 918 compartment is defined by assigning the initial and final state as *ergodynamic compartments*,  
 919  $H^+_{neg} \rightarrow H^+_{pos}$  or  $0 = -1 H^+_{neg} + 1 H^+_{pos}$ , related to work (erg = work) that must be performed to  
 920 lift the proton from a lower to a higher electrochemical potential or from the lower to the higher  
 921 ergodynamic compartment (Gnaiger 1993b).

922 In analogy to *vectorial* translocation, the direction of a *scalar* chemical reaction,  $A \rightarrow B$   
 923 or  $0 = -1 A + 1 B$ , is defined by assigning substrates and products, A and B, as ergodynamic  
 924 compartments.  $O_2$  is defined as a substrate in respiratory  $O_2$  consumption, which together with  
 925 the fuel substrates comprises the substrate compartment of the catabolic reaction. Volume-  
 926 specific scalar  $O_2$  flux is coupled to vectorial translocation, yielding the  $H^+_{pos}/O_2$  ratio (**Figure**  
 927 **2**).

---

### 928 929 3.2. Normalization for system-size: flux per chamber volume

930  
 931 **System-specific flux,  $J_{V,O_2}$ :** The experimental system (experimental chamber) is part of  
 932 the measurement apparatus, separated from the environment as an isolated, closed, open,  
 933 isothermal or non-isothermal system (**Table 4**). On another level, we distinguish between (1)  
 934 the *system* with volume  $V$  and mass  $m$  defined by the system boundaries, and (2) the *sample* or  
 935 *objects* with volume  $V_X$  and mass  $m_X$  which are enclosed in the experimental chamber (**Figure**  
 936 **6**). Metabolic  $O_2$  flow per object,  $I_{O_2/X}$ , increases as the mass of the object is increased. Sample  
 937 mass-specific  $O_2$  flux,  $J_{O_2/mX}$  should be independent of the mass of the sample studied in the  
 938 instrument chamber, but system volume-specific  $O_2$  flux,  $J_{V,O_2}$  (per volume of the instrument  
 939 chamber), should increase in direct proportion to the mass of the sample in the chamber.  
 940 Whereas  $J_{V,O_2}$  depends on mass-concentration of the sample in the chamber, it should be

941 independent of the chamber (system) volume at constant sample mass. There are practical  
 942 limitations to increase the mass-concentration of the sample in the chamber, when one is  
 943 concerned about crowding effects and instrumental time resolution.

944 When the reactor volume does not change during the reaction, which is typical for liquid  
 945 phase reactions, the volume-specific *flux of a chemical reaction*  $r$  is the time derivative of the  
 946 advancement of the reaction per unit volume,  $J_{V,rB} = d_r\zeta_B/dt \cdot V^{-1}$  [(mol·s<sup>-1</sup>)·L<sup>-1</sup>]. The *rate of*  
 947 *concentration change* is  $dc_B/dt$  [(mol·L<sup>-1</sup>)·s<sup>-1</sup>], where concentration is  $c_B = n_B/V$ . There is a  
 948 difference between (1)  $J_{V,rO_2}$  [mol·s<sup>-1</sup>·L<sup>-1</sup>] and (2) rate of concentration change [mol·L<sup>-1</sup>·s<sup>-1</sup>].  
 949 These merge to a single expression only in closed systems. In open systems, external fluxes  
 950 (such as O<sub>2</sub> supply) are distinguished from internal transformations (catabolic flux, O<sub>2</sub>  
 951 consumption). In a closed system, external flows of all substances are zero and O<sub>2</sub> consumption  
 952 (internal flow of catabolic reactions  $k$ ),  $I_{kO_2}$  [pmol·s<sup>-1</sup>], causes a decline of the amount of O<sub>2</sub> in  
 953 the system,  $n_{O_2}$  [nmol]. Normalization of these quantities for the volume of the system,  $V$  [L ≡  
 954 dm<sup>3</sup>], yields volume-specific O<sub>2</sub> flux,  $J_{V,kO_2} = I_{kO_2}/V$  [nmol·s<sup>-1</sup>·L<sup>-1</sup>], and O<sub>2</sub> concentration, [O<sub>2</sub>]  
 955 or  $c_{O_2} = n_{O_2}/V$  [μmol·L<sup>-1</sup> = μM = nmol·mL<sup>-1</sup>]. Instrumental background O<sub>2</sub> flux is due to external  
 956 flux into a non-ideal closed respirometer; then total volume-specific flux has to be corrected for  
 957 instrumental background O<sub>2</sub> flux—O<sub>2</sub> diffusion into or out of the instrumental chamber.  $J_{V,kO_2}$   
 958 is relevant mainly for methodological reasons and should be compared with the accuracy of  
 959 instrumental resolution of background-corrected flux, *e.g.*, ±1 nmol·s<sup>-1</sup>·L<sup>-1</sup> (Gnaiger 2001).  
 960 ‘Metabolic’ or catabolic indicates O<sub>2</sub> flux,  $J_{kO_2}$ , corrected for: (1) instrumental background O<sub>2</sub>  
 961 flux; (2) chemical background O<sub>2</sub> flux due to autoxidation of chemical components added to  
 962 the incubation medium; and (3) *Rox* for O<sub>2</sub>-consuming side reactions unrelated to the catabolic  
 963 pathway  $k$ .

### 964 3.3. Normalization: per sample

965 The challenges of measuring mitochondrial respiratory flux are matched by those of  
 966 normalization. Application of common and defined units is required for direct transfer of  
 967 reported results into a database. The second [s] is the *SI* unit for the base quantity *time*. It is also  
 968 the standard time-unit used in solution chemical kinetics. A rate may be considered as the  
 969 numerator and normalization as the complementary denominator, which are tightly linked in  
 970 reporting the measurements in a format commensurate with the requirements of a database.  
 971 Normalization (**Table 4**) is guided by physicochemical principles, methodological  
 972 considerations, and conceptual strategies (**Figure 7**).

973 **Sample concentration,  $C_{mX}$ :** Normalization for sample concentration is required to  
 974 report respiratory data. Considering a tissue or cells as the sample,  $X$ , the sample mass is  $m_X$   
 975 [mg], which is frequently measured as wet or dry weight,  $W_w$  or  $W_d$  [mg], respectively, or as  
 976 amount of tissue or cell protein,  $m_{\text{protein}}$ . In the case of permeabilized tissues, cells, and  
 977 homogenates, the sample concentration,  $C_{mX} = m_X/V$  [g·L<sup>-1</sup> = mg·mL<sup>-1</sup>], is the mass of the  
 978 subsample of tissue that is transferred into the instrument chamber.

979 **Mass-specific flux,  $J_{O_2/mX}$ :** Mass-specific flux is obtained by expressing respiration per  
 980 mass of sample,  $m_X$  [mg].  $X$  is the type of sample—isolated mitochondria, tissue homogenate,  
 981 permeabilized fibres or cells. Volume-specific flux is divided by mass concentration of  $X$ ,  $J_{O_2/mX}$   
 982 =  $J_{V,O_2}/C_{mX}$ ; or flow per cell is divided by mass per cell,  $J_{O_2/mcell} = I_{O_2/cell}/M_{cell}$ . If mass-specific  
 983 O<sub>2</sub> flux is constant and independent of sample size (expressed as mass), then there is no  
 984 interaction between the subsystems. A 1.5 mg and a 3.0 mg muscle sample respire at identical  
 985 mass-specific flux. Mass-specific O<sub>2</sub> flux, however, may change with the mass of a tissue  
 986 sample, cells or isolated mitochondria in the measuring chamber, in which the nature of the  
 987 interaction becomes an issue. Therefore, cell density must be optimized, particularly in  
 988 experiments carried out in wells, considering the confluency of the cell monolayer or clumps  
 989 of cells (Salabei *et al.* 2014).  
 990  
 991



**Table 4. Sample concentrations and normalization of flux.**

Expression	Symbol	Definition	Unit	Notes
<b>Sample</b>				
identity of sample	$X$	object: cell, tissue, animal, patient		
number of sample entities $X$	$N_X$	number of objects	x	
mass of sample $X$	$m_X$		kg	1
mass of object $X$	$M_X$	$M_X = m_X \cdot N_X^{-1}$	$\text{kg} \cdot \text{x}^{-1}$	1
<b>Mitochondria</b>				
mitochondria	mt	$X = \text{mt}$		
amount of mt-elements	$mtE$	quantity of mt-marker	mtEU	
<b>Concentrations</b>				
object number concentration	$C_{NX}$	$C_{NX} = N_X \cdot V^{-1}$	$\text{x} \cdot \text{m}^{-3}$	2
sample mass concentration	$C_{mX}$	$C_{mX} = m_X \cdot V^{-1}$	$\text{kg} \cdot \text{m}^{-3}$	
mitochondrial concentration	$C_{mtE}$	$C_{mtE} = mtE \cdot V^{-1}$	$\text{mtEU} \cdot \text{m}^{-3}$	3
specific mitochondrial density	$D_{mtE}$	$D_{mtE} = mtE \cdot m_X^{-1}$	$\text{mtEU} \cdot \text{kg}^{-1}$	4
mitochondrial content, $mtE$ per object $X$	$mtE_X$	$mtE_X = mtE \cdot N_X^{-1}$	$\text{mtEU} \cdot \text{x}^{-1}$	5
<b>O<sub>2</sub> flow and flux</b>				
flow, system	$I_{O_2}$	internal flow	$\text{mol} \cdot \text{s}^{-1}$	6
volume-specific flux	$J_{V,O_2}$	$J_{V,O_2} = I_{O_2} \cdot V^{-1}$	$\text{mol} \cdot \text{s}^{-1} \cdot \text{m}^{-3}$	7
flow per object $X$	$I_{O_2/X}$	$I_{O_2/X} = J_{V,O_2} \cdot C_{NX}^{-1}$	$\text{mol} \cdot \text{s}^{-1} \cdot \text{x}^{-1}$	8
mass-specific flux	$J_{O_2/mX}$	$J_{O_2/mX} = J_{V,O_2} \cdot C_{mX}^{-1}$	$\text{mol} \cdot \text{s}^{-1} \cdot \text{kg}^{-1}$	9
mitochondria-specific flux	$J_{O_2/mtE}$	$J_{O_2/mtE} = J_{V,O_2} \cdot C_{mtE}^{-1}$	$\text{mol} \cdot \text{s}^{-1} \cdot \text{mtEU}^{-1}$	10

- 994 1 The SI prefix k is used for the SI base unit of mass (kg = 1,000 g). In praxis, various SI prefixes are  
995 used for convenience, to make numbers easily readable, e.g., 1 mg tissue, cell or mitochondrial mass  
996 instead of 0.000001 kg.
- 997 2 In case sample  $X = \text{cells}$ , the object number concentration is  $C_{N_{\text{cell}}} = N_{\text{cell}} \cdot V^{-1}$ , and volume may be  
998 expressed in [ $\text{dm}^3 \equiv \text{L}$ ] or [ $\text{cm}^3 = \text{mL}$ ]. See **Table 5** for different object types.
- 999 3 mt-concentration is an experimental variable, dependent on sample concentration: (1)  $C_{mtE} = mtE \cdot V^{-1}$ ;  
1000 (2)  $C_{mtE} = mtE_X \cdot C_{NX}$ ; (3)  $C_{mtE} = C_{mX} \cdot D_{mtE}$ .
- 1001 4 If the amount of mitochondria,  $mtE$ , is expressed as mitochondrial mass, then  $D_{mtE}$  is the mass  
1002 fraction of mitochondria in the sample. If  $mtE$  is expressed as mitochondrial volume,  $V_{\text{mt}}$ , and the  
1003 mass of sample,  $m_X$ , is replaced by volume of sample,  $V_X$ , then  $D_{mtE}$  is the volume fraction of  
1004 mitochondria in the sample.
- 1005 5  $mtE_X = mtE \cdot N_X^{-1} = C_{mtE} \cdot C_{NX}^{-1}$ .
- 1006 6 O<sub>2</sub> can be replaced by other chemicals B to study different reactions, e.g., ATP, H<sub>2</sub>O<sub>2</sub>, or  
1007 compartmental translocations, e.g., Ca<sup>2+</sup>.
- 1008 7  $I_{O_2}$  and  $V$  are defined per instrument chamber as a system of constant volume (and constant  
1009 temperature), which may be closed or open.  $I_{O_2}$  is abbreviated for  $I_{r,O_2}$ , i.e., the metabolic or internal  
1010 O<sub>2</sub> flow of the chemical reaction  $r$  in which O<sub>2</sub> is consumed, hence the negative stoichiometric  
1011 number,  $\nu_{O_2} = -1$ .  $I_{r,O_2} = d_r n_{O_2} / dt \cdot \nu_{O_2}^{-1}$ . If  $r$  includes all chemical reactions in which O<sub>2</sub> participates, then  
1012  $d_r n_{O_2} = dn_{O_2} - d_e n_{O_2}$ , where  $dn_{O_2}$  is the change in the amount of O<sub>2</sub> in the instrument chamber and  $d_e n_{O_2}$   
1013 is the amount of O<sub>2</sub> added externally to the system. At steady state, by definition  $dn_{O_2} = 0$ , hence  $d_r n_{O_2}$   
1014  $= -d_e n_{O_2}$ .
- 1015 8  $J_{V,O_2}$  is an experimental variable, expressed per volume of the instrument chamber.
- 1016 9  $I_{O_2/X}$  is a physiological variable, depending on the size of entity  $X$ .
- 1017 10 There are many ways to normalize for a mitochondrial marker, that are used in different experimental  
1018 approaches: (1)  $J_{O_2/mtE} = J_{V,O_2} \cdot C_{mtE}^{-1}$ ; (2)  $J_{O_2/mtE} = J_{V,O_2} \cdot C_{mX}^{-1} \cdot D_{mtE}^{-1} = J_{O_2/mX} \cdot D_{mtE}^{-1}$ ; (3)  $J_{O_2/mtE} =$   
1019  $J_{V,O_2} \cdot C_{NX}^{-1} \cdot mtE_X^{-1} = I_{O_2/X} \cdot mtE_X^{-1}$ ; (4)  $J_{O_2/mtE} = I_{O_2} \cdot mtE^{-1}$ . The mt-elemental unit [mtEU] varies between  
1020 different mt-markers.



1021

**Table 5. Sample types, X, abbreviations, and quantification.**

Identity of sample	X	$N_X$	Mass <sup>a</sup>	Volume	mt-Marker
mitochondrial preparation	mt-prep	[x]	[kg]	[m <sup>3</sup> ]	[mtEU]
isolated mitochondria	imt		$m_{mt}$	$V_{mt}$	$mtE$
tissue homogenate	thom		$m_{thom}$		$mtE_{thom}$
permeabilized tissue	pti		$m_{pti}$		$mtE_{pti}$
permeabilized fibre	pfi		$m_{pfi}$		$mtE_{pfi}$
permeabilized cell	pce	$N_{pce}$	$M_{pce}$	$V_{pce}$	$mtE_{pce}$
cells <sup>b</sup>	cell	$N_{cell}$	$M_{cell}$	$V_{cell}$	$mtE_{cell}$
intact cell, viable cell	vce	$N_{vce}$	$M_{vce}$	$V_{vce}$	
dead cell	dce	$N_{dce}$	$M_{dce}$	$V_{dce}$	
organism	org	$N_{org}$	$M_{org}$	$V_{org}$	

1022

<sup>a</sup> Instead of mass, the wet weight or dry weight is frequently stated,  $W_w$  or  $W_d$ .

1023

$m_X$  is mass of the sample [kg],  $M_X$  is mass of the object [kg·x<sup>-1</sup>].

1024

<sup>b</sup> Total cell count,  $N_{cell} = N_{vce} + N_{dce}$

1025

1026

**Number concentration,  $C_{NX}$ :**  $C_{NX}$  is the experimental *number concentration* of sample X. In the case of cells or animals, e.g., nematodes,  $C_{NX} = N_X/V$  [x·L<sup>-1</sup>], where  $N_X$  is the number of cells or organisms in the chamber (**Table 4**).

1027

1028

1029

**Flow per object,  $I_{O_2/X}$ :** A special case of normalization is encountered in respiratory studies with permeabilized (or intact) cells. If respiration is expressed per cell, the O<sub>2</sub> flow per measurement system is replaced by the O<sub>2</sub> flow per cell,  $I_{O_2/cell}$  (**Table 4**). O<sub>2</sub> flow can be calculated from volume-specific O<sub>2</sub> flux,  $J_{V,O_2}$  [nmol·s<sup>-1</sup>·L<sup>-1</sup>] (per V of the measurement chamber [L]), divided by the number concentration of cells,  $C_{Ncell} = N_{cell}/V$  [cell·L<sup>-1</sup>], where  $N_{cell}$  is the number of cells in the chamber. The total cell count is the sum of viable and dead cells,  $N_{cell} = N_{vce} + N_{dce}$  (**Table 5**). The cell viability index,  $CVI = N_{vce}/N_{cell}$ , is the ratio of viable cells ( $N_{vce}$ ; before experimental permeabilization) per total cell count. After experimental permeabilization, all cells are permeabilized,  $N_{pce} = N_{cell}$ . The cell viability index can be used to normalize respiration for the number of cells that have been viable before experimental permeabilization,  $I_{O_2/vce} = I_{O_2/cell}/CVI$ , considering that mitochondrial respiratory dysfunction in dead cells should be eliminated as a confounding factor.

1030

1031

1032

1033

1034

1035

1036

1037

1038

1039

1040

Cellular O<sub>2</sub> flow can be compared between cells of identical size. To take into account changes and differences in cell size, normalization is required to obtain cell size-specific or mitochondrial marker-specific O<sub>2</sub> flux (Renner *et al.* 2003).

1041

1042

1043

1044

1045

1046

1047

1048

1049

1050

The complexity changes when the sample is a whole organism studied as an experimental model. The scaling law in respiratory physiology reveals a strong interaction of O<sub>2</sub> flow and individual body mass of an organism, since *basal* metabolic rate (flow) does not increase linearly with body mass, whereas *maximum* mass-specific O<sub>2</sub> flux,  $\dot{V}_{O_2max}$  or  $\dot{V}_{O_2peak}$ , is approximately constant across a large range of individual body mass (Weibel and Hoppeler 2005), with individuals, breeds, and species deviating substantially from this relationship.  $\dot{V}_{O_2peak}$  of human endurance athletes is 60 to 80 mL O<sub>2</sub>·min<sup>-1</sup>·kg<sup>-1</sup> body mass, converted to  $J_{O_2peak/M}$  of 45 to 60 nmol·s<sup>-1</sup>·g<sup>-1</sup> (Gnaiger 2014; **Table 6**).

1051

1052

1053

### 3.4. Normalization for mitochondrial content

1054

1055

1056

1057

1058

1059

1060

Tissues can contain multiple cell populations that may have distinct mitochondrial subtypes. Mitochondria undergo dynamic fission and fusion cycles, and can exist in multiple stages and sizes that may be altered by a range of factors. The isolation of mitochondria (often achieved through differential centrifugation) can therefore yield a subsample of the mitochondrial types present in a tissue, depending on the isolation protocols utilized (e.g., centrifugation speed). This possible bias should be taken into account when planning

1061 experiments using isolated mitochondria. Different sizes of mitochondria are enriched at  
 1062 specific centrifugation speeds, which can be used strategically for isolation of mitochondrial  
 1063 subpopulations.

1064 Part of the mitochondrial content of a tissue is lost during preparation of isolated  
 1065 mitochondria. The fraction of isolated mitochondria obtained from a tissue sample is expressed  
 1066 as mitochondrial recovery. At a high mitochondrial recovery the fraction of isolated  
 1067 mitochondria is more representative of the total mitochondrial population than in preparations  
 1068 characterized by low recovery. Determination of the mitochondrial recovery and yield is based  
 1069 on measurement of the concentration of a mitochondrial marker in the stock of isolated  
 1070 mitochondria,  $C_{mtE,stock}$ , and crude tissue homogenate,  $C_{mtE,thom}$ , which simultaneously provides  
 1071 information on the specific mitochondrial density in the sample,  $D_{mtE}$  (**Table 4**).

1072 Normalization is a problematic subject; it is essential to consider the question of the study.  
 1073 If the study aims at comparing tissue performance—such as the effects of a treatment on a  
 1074 specific tissue, then normalization for tissue mass or protein content is appropriate. However,  
 1075 if the aim is to find differences on mitochondrial function independent of mitochondrial density  
 1076 (**Table 4**), then normalization to a mitochondrial marker is imperative (**Figure 7**). One cannot  
 1077 assume that quantitative changes in various markers—such as mitochondrial proteins—  
 1078 necessarily occur in parallel with one another. It should be established that the marker chosen  
 1079 is not selectively altered by the performed treatment. In conclusion, the normalization must  
 1080 reflect the question under investigation to reach a satisfying answer. On the other hand, the goal  
 1081 of comparing results across projects and institutions requires standardization on normalization  
 1082 for entry into a databank.

1083

<b>Flow, Performance</b>	=	<b>Element function</b>	x	<b>Element density</b>	x	<b>Size of object</b>
$\frac{\text{mol}\cdot\text{s}^{-1}}{\text{x}}$	=	$\frac{\text{mol}\cdot\text{s}^{-1}}{x_{mtE}}$	·	$\frac{x_{mtE}}{\text{kg}}$	·	$\frac{\text{kg}}{\text{x}}$

<b>A</b>	<b>Flow</b>	=	<b>mt-specific flux</b>	x	<b>mt-structure, functional elements</b>
	$I_{O_2/X}$	=	$J_{O_2/mtE}$	·	$mtE_X$
					$\frac{mtE_X}{M_X} \cdot M_X$

	$I_{O_2/X}$	=	$J_{O_2/mtE}$	·	$D_{mtE}$	·	$M_X$
	$\frac{I_{O_2/X}}{M_X}$	=	$\frac{I_{O_2/X}}{mtE_X}$	·	$\frac{mtE_X}{M_X}$		

<b>B</b>	<b>Flow</b>	=	<b>Object mass- specific flux</b>	x	<b>Mass of object</b>
	$I_{O_2/X}$	=	$J_{O_2/MX}$	·	$M_X$

1084

1085 **Figure 7. Structure-function analysis of performance of an organism, organ or tissue, or**  
 1086 **a cell (sample entity,  $X$ )**

1087  $O_2$  flow,  $I_{O_2/X}$ , is the product of performance per functional element (element function,  
 1088 mitochondria-specific flux), element density (mitochondrial density,  $D_{mtE}$ ), and size of entity  $X$   
 1089 (mass,  $M_X$ ). (A) Structured analysis: performance is the product of mitochondrial *function* (mt-  
 1090 specific flux) and *structure* (functional elements;  $D_{mtE}$  times mass of  $X$ ). (B) Unstructured  
 1091 analysis: performance is the product of *entity mass-specific flux*,  $J_{O_2/MX} = I_{O_2/X}/M_X = I_{O_2}/m_X$   
 1092 [ $\text{mol}\cdot\text{s}^{-1}\cdot\text{kg}^{-1}$ ] and *size of entity*, expressed as mass of  $X$ ;  $M_X = m_X \cdot N_X^{-1}$  [ $\text{kg}\cdot\text{x}^{-1}$ ]. See **Table 4** for  
 1093 further explanation of quantities and units. Modified from Gnaiger (2014).

1094 **Mitochondrial concentration,  $C_{mtE}$ , and mitochondrial markers:** Mitochondrial  
 1095 organelles comprise a dynamic cellular reticulum in various states of fusion and fission. Hence,  
 1096 the definition of an "amount" of mitochondria is often misconceived: mitochondria cannot be  
 1097 counted reliably as a number of occurring elements. Therefore, quantification of the "amount"  
 1098 of mitochondria depends on the measurement of chosen mitochondrial markers. 'Mitochondria  
 1099 are the structural and functional elemental units of cell respiration' (Gnaiger 2014). The  
 1100 quantity of a mitochondrial marker can reflect the amount of *mitochondrial elements*,  $mtE$ ,  
 1101 expressed in various mitochondrial elemental units [mtEU] specific for each measured mt-  
 1102 marker (**Table 4**). However, since mitochondrial quality may change in response to stimuli—  
 1103 particularly in mitochondrial dysfunction and after exercise training (Pesta *et al.* 2011; Campos  
 1104 *et al.* 2017)—some markers can vary while others are unchanged: (1) Mitochondrial volume  
 1105 and membrane area are structural markers, whereas mitochondrial protein mass is frequently  
 1106 used as a marker for isolated mitochondria. (2) Molecular and enzymatic mitochondrial markers  
 1107 (amounts or activities) can be selected as matrix markers, *e.g.*, citrate synthase activity, mtDNA;  
 1108 mtIM-markers, *e.g.*, cytochrome *c* oxidase activity, *aa*<sub>3</sub> content, cardiolipin, or mtOM-markers,  
 1109 *e.g.*, TOM20. (3) Extending the measurement of mitochondrial marker enzyme activity to  
 1110 mitochondrial pathway capacity, ET- or OXPHOS-capacity can be considered as an integrative  
 1111 functional mitochondrial marker.

1112 Depending on the type of mitochondrial marker, the mitochondrial elements,  $mtE$ , are  
 1113 expressed in marker-specific units. Mitochondrial concentration in the measurement chamber  
 1114 and the tissue of origin are quantified as (1) a quantity for normalization in functional analyses,  
 1115  $C_{mtE}$ , and (2) a physiological output that is the result of mitochondrial biogenesis and  
 1116 degradation,  $D_{mtE}$ , respectively (**Table 4**). It is recommended, therefore, to distinguish  
 1117 *experimental mitochondrial concentration*,  $C_{mtE} = mtE/V$  and *physiological mitochondrial*  
 1118 *density*,  $D_{mtE} = mtE/m_X$ . Then mitochondrial density is the amount of mitochondrial elements  
 1119 per mass of tissue, which is a biological variable (**Figure 7**). The experimental variable is  
 1120 mitochondrial density multiplied by sample mass concentration in the measuring chamber,  $C_{mtE}$   
 1121  $= D_{mtE} \cdot C_{mX}$ , or mitochondrial content multiplied by sample number concentration,  $C_{mtE} =$   
 1122  $mtE_X \cdot C_{NX}$  (**Table 4**).

1123 **Mitochondria-specific flux,  $J_{O_2/mtE}$ :** Volume-specific metabolic O<sub>2</sub> flux depends on: (1)  
 1124 the sample concentration in the volume of the instrument chamber,  $C_{mX}$ , or  $C_{NX}$ ; (2) the  
 1125 mitochondrial density in the sample,  $D_{mtE} = mtE/m_X$  or  $mtE_X = mtE/N_X$ ; and (3) the specific  
 1126 mitochondrial activity or performance per elemental mitochondrial unit,  $J_{O_2/mtE} = J_{V,O_2}/C_{mtE}$   
 1127 [mol·s<sup>-1</sup>·mtEU<sup>-1</sup>] (**Table 4**). Obviously, the numerical results for  $J_{O_2/mtE}$  vary with the type of  
 1128 mitochondrial marker chosen for measurement of  $mtE$  and  $C_{mtE} = mtE/V$  [mtEU·m<sup>-3</sup>].

1129

### 1130 3.5. Evaluation of mitochondrial markers

1131

1132 Different methods are implicated in the quantification of mitochondrial markers and have  
 1133 different strengths. Some problems are common for all mitochondrial markers,  $mtE$ : (1)  
 1134 Accuracy of measurement is crucial, since even a highly accurate and reproducible  
 1135 measurement of O<sub>2</sub> flux results in an inaccurate and noisy expression if normalized by a biased  
 1136 and noisy measurement of a mitochondrial marker. This problem is acute in mitochondrial  
 1137 respiration because the denominators used (the mitochondrial markers) are often small moieties  
 1138 of which accurate and precise determination is difficult. This problem can be avoided when O<sub>2</sub>  
 1139 fluxes measured in substrate-uncoupler-inhibitor titration protocols are normalized for flux in  
 1140 a defined respiratory reference state, which is used as an *internal* marker and yields flux control  
 1141 ratios, *FCRs*. *FCRs* are independent of *externally* measured markers and, therefore, are  
 1142 statistically robust, considering the limitations of ratios in general (Jasienski and Bazzaz 1999).  
 1143 *FCRs* indicate qualitative changes of mitochondrial respiratory control, with highest  
 1144 quantitative resolution, separating the effect of mitochondrial density or concentration on  $J_{O_2/mX}$

1145 and  $I_{O_2/X}$  from that of function per elemental mitochondrial marker,  $J_{O_2}/mtE$  (Pesta *et al.* 2011;  
 1146 Gnaiger 2014). (2) If mitochondrial quality does not change and only the amount of  
 1147 mitochondria varies as a determinant of mass-specific flux, any marker is equally qualified in  
 1148 principle; then in practice selection of the optimum marker depends only on the accuracy and  
 1149 precision of measurement of the mitochondrial marker. (3) If mitochondrial flux control ratios  
 1150 change, then there may not be any best mitochondrial marker. In general, measurement of  
 1151 multiple mitochondrial markers enables a comparison and evaluation of normalization for a  
 1152 variety of mitochondrial markers. Particularly during postnatal development, the activity of  
 1153 marker enzymes—such as cytochrome *c* oxidase and citrate synthase—follows different time  
 1154 courses (Drahota *et al.* 2004). Evaluation of mitochondrial markers in healthy controls is  
 1155 insufficient for providing guidelines for application in the diagnosis of pathological states and  
 1156 specific treatments.

1157 In line with the concept of the respiratory control ratio (Chance and Williams 1955a), the  
 1158 most readily used normalization is that of flux control ratios and flux control factors (Gnaiger  
 1159 2014). Selection of the state of maximum flux in a protocol as the reference state has the  
 1160 advantages of: (1) internal normalization; (2) statistical linearization of the response in the range  
 1161 of 0 to 1; and (3) consideration of maximum flux for integrating a large number of elemental  
 1162 steps in the OXPHOS- or ET-pathways. This reduces the risk of selecting a functional marker  
 1163 that is specifically altered by the treatment or pathology, yet increases the chance that the highly  
 1164 integrative pathway is disproportionately affected, *e.g.*, the OXPHOS- rather than ET-pathway  
 1165 in case of an enzymatic defect in the phosphorylation-pathway. In this case, additional  
 1166 information can be obtained by reporting flux control ratios based on a reference state which  
 1167 indicates stable tissue-mass specific flux. Stereological determination of mitochondrial content  
 1168 via two-dimensional transmission electron microscopy can have limitations due to the dynamics  
 1169 of mitochondrial size (Meinild Lundby *et al.* 2017). Accurate determination of three-  
 1170 dimensional volume by two-dimensional microscopy can be both time consuming and  
 1171 statistically challenging (Larsen *et al.* 2012).

1172 The validity of using mitochondrial marker enzymes (citrate synthase activity, Complex  
 1173 I–IV amount or activity) for normalization of flux is limited in part by the same factors that  
 1174 apply to flux control ratios. Strong correlations between various mitochondrial markers and  
 1175 citrate synthase activity (Reichmann *et al.* 1985; Boushel *et al.* 2007; Mogensen *et al.* 2007)  
 1176 are expected in a specific tissue of healthy subjects and in disease states not specifically  
 1177 targeting citrate synthase. Citrate synthase activity is acutely modifiable by exercise  
 1178 (Tonkonogi *et al.* 1997; Leek *et al.* 2001). Evaluation of mitochondrial markers related to a  
 1179 selected age and sex cohort cannot be extrapolated to provide recommendations for  
 1180 normalization in respirometric diagnosis of disease, in different states of development and  
 1181 ageing, different cell types, tissues, and species. mtDNA normalized to nDNA via qPCR is  
 1182 correlated to functional mitochondrial markers including OXPHOS- and ET-capacity in some  
 1183 cases (Puntschart *et al.* 1995; Wang *et al.* 1999; Menshikova *et al.* 2006; Boushel *et al.* 2007),  
 1184 but lack of such correlations have been reported (Menshikova *et al.* 2005; Schultz and Wiesner  
 1185 2000; Pesta *et al.* 2011). Several studies indicate a strong correlation between cardiolipin  
 1186 content and increase in mitochondrial function with exercise (Menshikova *et al.* 2005;  
 1187 Menshikova *et al.* 2007; Larsen *et al.* 2012; Faber *et al.* 2014), but it has not been evaluated as  
 1188 a general mitochondrial biomarker in disease.

### 1189 3.6. Conversion: units

1190  
 1191  
 1192 Many different units have been used to report the  $O_2$  consumption rate, OCR (**Table 6**).  
 1193 *SI* base units provide the common reference to introduce the theoretical principles (**Figure 6**),  
 1194 and are used with appropriately chosen *SI* prefixes to express numerical data in the most  
 1195 practical format, with an effort towards unification within specific areas of application (**Table**

1196 7). Reporting data in *SI* units—including the mole [mol], coulomb [C], joule [J], and second  
1197 [s]—should be encouraged, particularly by journals which propose the use of *SI* units.

1198  
1199

1200 **Table 6. Conversion of various units used in respirometry and**  
1201 **ergometry.**  $e^-$  is the number of electrons or reducing equivalents.  $z_B$  is the  
1202 charge number of entity B.  
1203

1 Unit	x	Multiplication factor	<i>SI</i> -unit	Note
ng.atom O·s <sup>-1</sup>	(2 e <sup>-</sup> )	0.5	nmol O <sub>2</sub> ·s <sup>-1</sup>	
ng.atom O·min <sup>-1</sup>	(2 e <sup>-</sup> )	8.33	pmol O <sub>2</sub> ·s <sup>-1</sup>	
natom O·min <sup>-1</sup>	(2 e <sup>-</sup> )	8.33	pmol O <sub>2</sub> ·s <sup>-1</sup>	
nmol O <sub>2</sub> ·min <sup>-1</sup>	(4 e <sup>-</sup> )	16.67	pmol O <sub>2</sub> ·s <sup>-1</sup>	
nmol O <sub>2</sub> ·h <sup>-1</sup>	(4 e <sup>-</sup> )	0.2778	pmol O <sub>2</sub> ·s <sup>-1</sup>	
mL O <sub>2</sub> ·min <sup>-1</sup> at STPD <sup>a</sup>		0.744	μmol O <sub>2</sub> ·s <sup>-1</sup>	1
W = J/s at -470 kJ/mol O <sub>2</sub>		-2.128	μmol O <sub>2</sub> ·s <sup>-1</sup>	
mA = mC·s <sup>-1</sup>	(z <sub>H+</sub> = 1)	10.36	nmol H <sup>+</sup> ·s <sup>-1</sup>	2
mA = mC·s <sup>-1</sup>	(z <sub>O<sub>2</sub></sub> = 4)	2.59	nmol O <sub>2</sub> ·s <sup>-1</sup>	2
nmol H <sup>+</sup> ·s <sup>-1</sup>	(z <sub>H+</sub> = 1)	0.09649	mA	3
nmol O <sub>2</sub> ·s <sup>-1</sup>	(z <sub>O<sub>2</sub></sub> = 4)	0.38594	mA	3

1204 1 At standard temperature and pressure dry (STPD: 0 °C = 273.15 K and 1 atm =  
1205 101.325 kPa = 760 mmHg), the molar volume of an ideal gas,  $V_m$ , and  $V_{m,O_2}$  is  
1206 22.414 and 22.392 L·mol<sup>-1</sup>, respectively. Rounded to three decimal places, both  
1207 values yield the conversion factor of 0.744. For comparison at normal  
1208 temperature and pressure dry (NTPD: 20 °C),  $V_{m,O_2}$  is 24.038 L·mol<sup>-1</sup>. Note that  
1209 the *SI* standard pressure is 100 kPa.

1210 2 The multiplication factor is  $10^6/(z_B \cdot F)$ .

1211 3 The multiplication factor is  $z_B \cdot F/10^6$ .

1212  
1213

1214 Although volume is expressed as m<sup>3</sup> using the *SI* base unit, the litre [dm<sup>3</sup>] is a  
1215 conventional unit of volume for concentration and is used for most solution chemical kinetics.  
1216 If one multiplies  $I_{O_2/cell}$  by  $C_{Ncell}$ , then the result will not only be the amount of O<sub>2</sub> [mol]  
1217 consumed per time [s<sup>-1</sup>] in one litre [L<sup>-1</sup>], but also the change in O<sub>2</sub> concentration per second  
1218 (for any volume of an ideally closed system). This is ideal for kinetic modeling as it blends with  
1219 chemical rate equations where concentrations are typically expressed in mol·L<sup>-1</sup> (Wagner *et al.*  
1220 2011). In studies of multinuclear cells—such as differentiated skeletal muscle cells—it is easy  
1221 to determine the number of nuclei but not the total number of cells. A generalized concept,  
1222 therefore, is obtained by substituting cells by nuclei as the sample entity. This does not hold,  
1223 however, for enucleated platelets.

1224 For studies of cells, we recommend that respiration be expressed, as far as possible, as:  
1225 (1) O<sub>2</sub> flux normalized for a mitochondrial marker, for separation of the effects of mitochondrial  
1226 quality and content on cell respiration (this includes *FCRs* as a normalization for a functional  
1227 mitochondrial marker); (2) O<sub>2</sub> flux in units of cell volume or mass, for comparison of respiration  
1228 of cells with different cell size (Renner *et al.* 2003) and with studies on tissue preparations, and  
1229 (3) O<sub>2</sub> flow in units of attomole (10<sup>-18</sup> mol) of O<sub>2</sub> consumed in a second by each cell  
1230 [amol·s<sup>-1</sup>·cell<sup>-1</sup>], numerically equivalent to [pmol·s<sup>-1</sup>·10<sup>-6</sup> cells]. This convention allows  
1231 information to be easily used when designing experiments in which O<sub>2</sub> flow must be considered.  
1232 For example, to estimate the volume-specific O<sub>2</sub> flux in an instrument chamber that would be



1233 expected at a particular cell number concentration, one simply needs to multiply the flow per  
 1234 cell by the number of cells per volume of interest. This provides the amount of O<sub>2</sub> [mol]  
 1235 consumed per time [s<sup>-1</sup>] per unit volume [L<sup>-1</sup>]. At an O<sub>2</sub> flow of 100 amol·s<sup>-1</sup>·cell<sup>-1</sup> and a cell  
 1236 density of 10<sup>9</sup> cells·L<sup>-1</sup> (10<sup>6</sup> cells·mL<sup>-1</sup>), the volume-specific O<sub>2</sub> flux is 100 nmol·s<sup>-1</sup>·L<sup>-1</sup> (100  
 1237 pmol·s<sup>-1</sup>·mL<sup>-1</sup>).  
 1238  
 1239

**Table 7. Conversion of units with preservation of numerical values.**

Name	Frequently used unit	Equivalent unit	Note
volume-specific flux, $J_{V,O_2}$	pmol·s <sup>-1</sup> ·mL <sup>-1</sup> mmol·s <sup>-1</sup> ·L <sup>-1</sup>	nmol·s <sup>-1</sup> ·L <sup>-1</sup> mol·s <sup>-1</sup> ·m <sup>-3</sup>	1
cell-specific flow, $I_{O_2/cell}$	pmol·s <sup>-1</sup> ·10 <sup>-6</sup> cells	amol·s <sup>-1</sup> ·cell <sup>-1</sup>	2
	pmol·s <sup>-1</sup> ·10 <sup>-9</sup> cells	zmol·s <sup>-1</sup> ·cell <sup>-1</sup>	3
cell number concentration, $C_{Nce}$	10 <sup>6</sup> cells·mL <sup>-1</sup>	10 <sup>9</sup> cells·L <sup>-1</sup>	
mitochondrial protein concentration, $C_{mtE}$	0.1 mg·mL <sup>-1</sup>	0.1 g·L <sup>-1</sup>	
mass-specific flux, $J_{O_2/m}$	pmol·s <sup>-1</sup> ·mg <sup>-1</sup>	nmol·s <sup>-1</sup> ·g <sup>-1</sup>	4
catabolic power, $P_k$	μW·10 <sup>-6</sup> cells	pW·cell <sup>-1</sup>	1
volume	1,000 L	m <sup>3</sup> (1,000 kg)	
	L	dm <sup>3</sup> (kg)	
	mL	cm <sup>3</sup> (g)	
	μL	mm <sup>3</sup> (mg)	
	fL	μm <sup>3</sup> (pg)	5
amount of substance concentration	M = mol·L <sup>-1</sup>	mol·dm <sup>-3</sup>	

1240

1241 1 pmol: picomole = 10<sup>-12</sup> mol1242 2 amol: attomole = 10<sup>-18</sup> mol1243 3 zmol: zeptomole = 10<sup>-21</sup> mol

1244

1245 ET-capacity in human cell types including HEK 293, primary HUVEC and fibroblasts  
 1246 ranges from 50 to 180 amol·s<sup>-1</sup>·cell<sup>-1</sup>, measured in intact cells in the noncoupled state (see  
 1247 Gnaiger 2014). At 100 amol·s<sup>-1</sup>·cell<sup>-1</sup> corrected for *Rox*, the current across the mt-membranes,  
 1248  $I_{H^+e}$ , approximates 193 pA·cell<sup>-1</sup> or 0.2 nA per cell. See Rich (2003) for an extension of  
 1249 quantitative bioenergetics from the molecular to the human scale, with a transmembrane proton  
 1250 flux equivalent to 520 A in an adult at a catabolic power of -110 W. Modelling approaches  
 1251 illustrate the link between protonmotive force and currents (Willis *et al.* 2016).

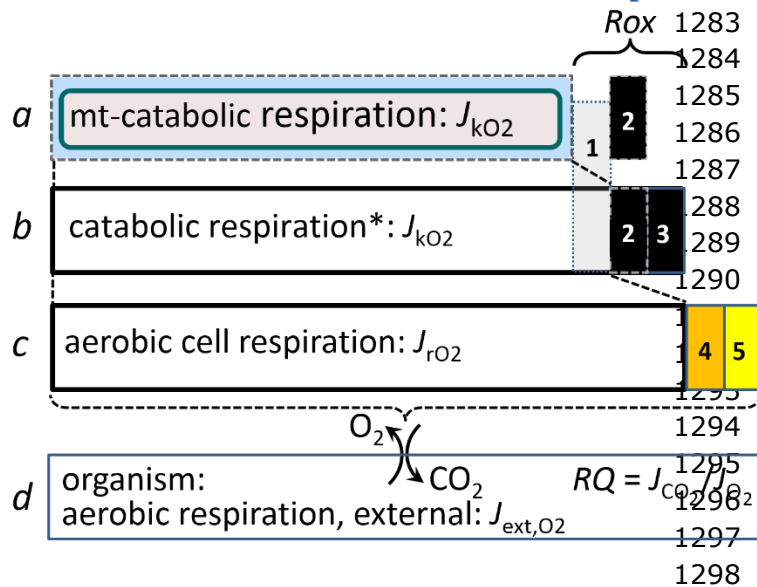
1252 We consider isolated mitochondria as powerhouses and proton pumps as molecular  
 1253 machines to relate experimental results to energy metabolism of the intact cell. The cellular  
 1254 P<sub>»</sub>/O<sub>2</sub> based on oxidation of glycogen is increased by the glycolytic (fermentative) substrate-  
 1255 level phosphorylation of 3 P<sub>»</sub>/Glyc or 0.5 mol P<sub>»</sub> for each mol O<sub>2</sub> consumed in the complete  
 1256 oxidation of a mol glycosyl unit (Glyc). Adding 0.5 to the mitochondrial P<sub>»</sub>/O<sub>2</sub> ratio of 5.4  
 1257 yields a bioenergetic cell physiological P<sub>»</sub>/O<sub>2</sub> ratio close to 6. Two NADH equivalents are  
 1258 formed during glycolysis and transported from the cytosol into the mitochondrial matrix, either  
 1259 by the malate-aspartate shuttle or by the glycerophosphate shuttle (**Figure 1**) resulting in  
 1260 different theoretical yields of ATP generated by mitochondria, the energetic cost of which  
 1261 potentially must be taken into account. Considering also substrate-level phosphorylation in the  
 1262 TCA cycle, this high P<sub>»</sub>/O<sub>2</sub> ratio not only reflects proton translocation and OXPHOS studied  
 1263 in isolation, but integrates mitochondrial physiology with energy transformation in the living  
 1264 cell (Gnaiger 1993a).  
 1265  
 1266

#### 4. Conclusions

MitoEAGLE can serve as a gateway to better diagnose mitochondrial respiratory defects linked to genetic variation, age-related health risks, sex-specific mitochondrial performance, lifestyle with its effects on degenerative diseases, and thermal and chemical environment. The present recommendations on coupling control states and rates, linked to the concept of the protonmotive force, are focused on studies with mitochondrial preparations. These will be extended in a series of reports on pathway control of mitochondrial respiration, respiratory states in intact cells, and harmonization of experimental procedures.

OXPHOS analysis is based on the study of mitochondrial preparations complementary to bioenergetic investigations of intact cells and organisms—from animal models to healthy persons or patients. Metabolic fluxes measured in defined coupling and pathway control states provide insights into the meaning of cellular and organismic respiration. An  $O_2$  flux balance scheme illustrates the relationships and general definitions (**Box 3**).

#### Box 3: Definitions: mitochondrial and cell respiration



**Mitochondrial respiration with reduction of oxygen catalysed by the electron transfer system (catabolic, a), catabolic respiration (including non-mitochondrial oxidation reactions, b), and oxygen balance of internal (c) and external (d) respiration**

All chemical reactions,  $r$ , that consume  $O_2$  in the cells of an organism, contribute to cell respiration,  $J_{rO_2}$ . (1) Non-mitochondrial contribution to  $O_2$  consumption by catabolic reactions, particularly

peroxisomal oxidases (\* the reactions  $k$  have to be defined specifically for  $a$  and  $b$ ; **Figure 1**); (2) mitochondrial residual oxygen consumption,  $Rox$ , after blocking the electron transfer system; (3) non-mitochondrial  $Rox$ ; (4) extracellular  $O_2$  consumption; (5) aerobic microbial respiration. Bars are not at a quantitative scale.

- a Mitochondrial catabolic respiration**,  $J_{kO_2}$ , is the  $O_2$  consumption by the ETS (**Figure 2**), excluding  $Rox$ .
- b Catabolic respiration**,  $J_{kO_2}$ , is the  $O_2$  consumption associated with catabolic pathways in the cell, including mitochondrial and peroxisomal oxidation reactions.
- c Aerobic cell respiration**,  $J_{rO_2}$ , takes into account internal  $O_2$ -consuming reactions,  $r$ , including  $Rox$ . In aerobic cell respiration, redox balance is maintained by the use of  $O_2$  as electron acceptor. Internal respiration of an organism includes extracellular  $O_2$  consumption and aerobic respiration by the microbiome. In general, respiration is distinguished from fermentation by: (1) the use of external electron acceptors for the maintenance of redox balance, whereas fermentation is characterized by the use of an internal electron acceptor produced in intermediary metabolism; and (2) compartmental coupling in vectorial oxidative phosphorylation, in contrast to exclusively scalar substrate-level phosphorylation in fermentation.
- d External respiration** balances internal respiration at steady-state, with circulation of the externally exchanged  $O_2$  between tissues and diffusion across cell membranes.  $O_2$  is

1318 transported from the environment across the respiratory cascade to the intracellular  
 1319 compartment, while bicarbonate and CO<sub>2</sub> are transported in reverse to the extracellular  
 1320 milieu and the organismic environment. Hemoglobin provides the molecular paradigm for  
 1321 the combination of O<sub>2</sub> and CO<sub>2</sub> exchange, as do lungs and gills on the morphological  
 1322 level. The respiratory quotient,  $RQ$ , is the molar CO<sub>2</sub>/O<sub>2</sub> exchange ratio; when combined  
 1323 with the respiratory nitrogen quotient, N/O<sub>2</sub>, the  $RQ$  reflects the proportion of  
 1324 carbohydrate, lipid and protein utilized in cell respiration during aerobically balanced  
 1325 steady-states.

---

1326

1327 Cell respiration is the process of exergonic and exothermic energy transformation in  
 1328 which scalar redox reactions are coupled to vectorial ion translocation across a semipermeable  
 1329 membrane, which separates the small volume of a bacterial cell or mitochondrion from the  
 1330 larger volume of its surroundings. The electrochemical exergy can be partially conserved in the  
 1331 phosphorylation of ADP to ATP or in ion pumping, or dissipated in an electrochemical short-  
 1332 circuit. Respiration is thus clearly distinguished from fermentation as the counterpart of cellular  
 1333 core energy metabolism. Respiration is separated in mitochondrial preparations from the  
 1334 interactions with the fermentative pathways of the intact cell.

1335 The optimal choice for expressing mitochondrial and cell respiration as O<sub>2</sub> flow per  
 1336 biological sample, and normalization for specific tissue-markers (volume, mass, protein) and  
 1337 mitochondrial markers (volume, protein, content, mtDNA, activity of marker enzymes,  
 1338 respiratory reference state) is guided by the scientific question under study. Interpretation of  
 1339 the data depends critically on appropriate normalization.

1340 We recommend for studies with mitochondrial preparations:

- 1341 • Normalization of respiratory rates should be provided as far as possible: (1) biophysical  
 1342 normalization: on a per cell basis as O<sub>2</sub> flow (may not be possible when dealing with  
 1343 tissues); (2) cellular normalization: per g cell or tissue protein, or per cell or tissue mass  
 1344 as mass-specific O<sub>2</sub> flux; and (3) mitochondrial normalization: per mitochondrial marker  
 1345 as mt-specific flux. With information on cell size and the use of multiple normalizations,  
 1346 maximum potential information is available (Renner *et al.* 2003; Wagner *et al.* 2011;  
 1347 Gnaiger 2014). Reporting flow in a respiratory chamber [nmol·s<sup>-1</sup>] is discouraged, since  
 1348 it restricts the analysis to intra-experimental comparison of relative (qualitative)  
 1349 differences.
- 1350 • Catabolic mitochondrial respiration is distinguished from residual oxygen consumption.  
 1351 Fluxes in mitochondrial coupling states should be, as far as possible, corrected for residual  
 1352 oxygen consumption.
- 1353 • In studies of isolated mitochondria, the mitochondrial recovery and yield should be  
 1354 reported. Experimental criteria for evaluation of purity versus integrity should be  
 1355 considered. Mitochondrial markers—such as citrate synthase activity as an enzymatic  
 1356 matrix marker—provide a link to the tissue of origin on the basis of calculating the  
 1357 mitochondrial recovery, *i.e.*, the fraction of mitochondrial marker obtained from a unit  
 1358 mass of tissue. Total mitochondrial protein is frequently applied as a mitochondrial  
 1359 marker, which is restricted to isolated mitochondria.
- 1360 • In studies of permeabilized cells, the viability of the cell culture or cell suspension of  
 1361 origin should be reported. Normalization should be evaluated for total cell count or viable  
 1362 cell count.
- 1363 • Terms and symbols are summarized in **Table 8**. Their use will facilitate transdisciplinary  
 1364 communication and support further developments towards a consistent theory of  
 1365 bioenergetics and mitochondrial physiology.
- 1366 • Technical terms related to and defined with normal words can be used as index terms in  
 1367 databases, support the creation of ontologies towards semantic information processing  
 1368 (MitoPedia), and help in communicating analytical findings as impactful data-driven

1369 stories. ‘*Making data available without making it understandable may be worse than not*  
 1370 *making it available at all*’ (National Academies of Sciences, Engineering, and Medicine  
 1371 2018). Success will depend on taking next steps: (1) exhaustive text-mining considering  
 1372 Omics data and functional data; (2) network analysis of Omics data with bioinformatics  
 1373 tools; (3) cross-validation with distinct bioinformatics approaches; (4) correlation with  
 1374 functional data; (5) guidelines for biological validation of network data. This is a call to  
 1375 carefully contribute to FAIR principles (Findable, Accessible, Interoperable, Reusable)  
 1376 for the sharing of scientific data.



1378 **Table 8. Terms, symbols, and units.**

Term	Symbol	Unit	Links and comments
1383			
1384	alternative quinol oxidase	AOX	Figure 2A
1385	amount of substance B	$n_B$	[mol]
1386	catabolic reaction	k	Figure 2, Box 3
1387	catabolic respiration	$J_{kO_2}$	varies Figure 2, Box 3
1388	cell number	$N_{cell}$	[x] Table 5; $N_{cell} = N_{vce} + N_{dce}$
1389	cell respiration	$J_{rO_2}$	varies Box 3
1390	cell viability index	CVI	$CVI = N_{vce}/N_{cell} = 1 - N_{dce}/N_{cell}$
1391	Complexes I to IV	CI to CIV	respiratory ET Complexes; Figure 2A
1392	concentration of substance B	$c_B = n_B \cdot V^{-1}$ ; [B]	[mol·m <sup>-3</sup> ] Box 2
1393	dead cell number	$N_{dce}$	[x] Table 5; non-viable cells, loss of plasma membrane barrier function
1394			
1395	electron transfer system	ETS	Figure 2A, Figure 4
1396	flow, for substance B	$I_B$	[mol·s <sup>-1</sup> ] system-related extensive quantity; Figure 6
1397			
1398	flux, for substance B	$J_B$	varies size-specific quantity; Figure 6
1399	inorganic phosphate	$P_i$	Figure 2C
1400	intact cell number, viable cell number	$N_{vce}$	[x] Table 5; viable cells, intact of plasma membrane barrier function
1401			
1402	LEAK	LEAK	Table 1, Figure 4
1403	mass of sample X	$m_X$	[kg] Table 4
1404	mass of entity X	$M_X$	[kg] mass of object X; Table 4
1405	MITOCARTA		<a href="https://www.broadinstitute.org/scientific-community/science/programs/metabolic-disease-program/publications/mitocarta/mitocarta-in-0">https://www.broadinstitute.org/scientific-community/science/programs/metabolic-disease-program/publications/mitocarta/mitocarta-in-0</a>
1406			
1407			
1408			
1409			
1410	MitoPedia		<a href="http://www.bioblast.at/index.php/MitoPedia">http://www.bioblast.at/index.php/MitoPedia</a>
1411	mitochondria or mitochondrial	mt	Box 1
1412	mitochondrial DNA	mtDNA	Box 1
1413	mitochondrial concentration	$C_{mtE} = mtE \cdot V^{-1}$	[mtEU·m <sup>-3</sup> ] Table 4
1414	mitochondrial content	$mtE_X = mtE \cdot N_X^{-1}$	[mtEU·x <sup>-1</sup> ] Table 4
1415	mitochondrial elemental unit	mtEU	varies Table 4, specific units for mt-marker
1416	mitochondrial inner membrane	mtIM	Figure 1; MIM is widely used; the first M is replaced by mt; Box 1
1417			
1418	mitochondrial outer membrane	mtOM	Figure 1; MOM is widely used; the first M is replaced by mt; Box 1
1419			
1420	mitochondrial recovery	$Y_{mtE}$	fraction of <i>mtE</i> recovered in sample from the tissue of origin
1421			
1422	mitochondrial yield	$Y_{mtE/m}$	$Y_{mtE/m} = Y_{mtE} \cdot D_{mtE}$ Figure 2C
1423	negative	neg	Figure 2C
1424	number concentration of X	$C_{NX}$	[x·m <sup>-3</sup> ] Table 4
1425	number of entities X	$N_X$	[x] Table 4, Figure 7
1426	number of entity B	$N_B$	[x] Table 4
1427	oxidative phosphorylation	OXPPOS	Table 1, Figure 4
1428	oxygen concentration	$c_{O_2} = n_{O_2} \cdot V^{-1}$ ; [O <sub>2</sub> ]	[mol·m <sup>-3</sup> ] Section 3.2



1429	oxygen flux, in reaction $r$	$J_{rO_2}$	<i>varies</i>	Box 3
1430	permeabilized cell number	$N_{pce}$	[x]	Table 5; experimental permeabilization of plasma membrane; $N_{pce} = N_{cell}$
1431				
1432	phosphorylation of ADP to ATP	$P_{\gg}$		Section 2.2
1433	positive	pos		Figure 2C
1434	proton in the negative compartment	$H^{+neg}$		Figure 2C
1435	proton in the positive compartment	$H^{+pos}$		Figure 2C
1436	rate of electron transfer in ET state	$E$		ET-capacity; Table 1
1437	rate of LEAK respiration	$L$		Table 1
1438	rate of oxidative phosphorylation	$P$		OXPHOS capacity; Table 1
1439	rate of residual oxygen consumption	$ROx$		Table 1
1440	residual oxygen consumption	ROX		Table 1
1441	respiratory supercomplex	SC I <sub>n</sub> III <sub>n</sub> IV <sub>n</sub>		Box 1; supramolecular assemblies composed of variable copy numbers ( $n$ ) of CI, CIII and CIV
1442				
1443				
1444	specific mitochondrial density	$D_{mtE} = mtE \cdot m_X^{-1}$	[mtEU·kg <sup>-1</sup> ]	Table 4
1445	volume	$V$	[m <sup>3</sup> ]	Table 7
1446	weight, dry weight	$W_d$	[kg]	used as mass of sample $X$ ; Figure 6
1447	weight, wet weight	$W_w$	[kg]	used as mass of sample $X$ ; Figure 6
1448				

1449

1450

## 1451 Acknowledgements

1452 We thank M. Beno for management assistance. Supported by COST Action CA15203  
1453 MitoEAGLE and K-Regio project MitoFit (E.G.).

1454

1455 **Competing financial interests:** E.G. is founder and CEO of Oroboros Instruments, Innsbruck,  
1456 Austria.

1457

1458

## 1459 5. References

1460

1461 Altmann R (1894) Die Elementarorganismen und ihre Beziehungen zu den Zellen. Zweite vermehrte Auflage.  
1462 Verlag Von Veit & Comp, Leipzig:160 pp.

1463 Beard DA (2005) A biophysical model of the mitochondrial respiratory system and oxidative phosphorylation.  
1464 PLoS Comput Biol 1(4):e36.

1465 Benda C (1898) Weitere Mitteilungen über die Mitochondria. Verh Dtsch Physiol Ges:376-83.

1466 Birkedal R, Laasmaa M, Vendelin M (2014) The location of energetic compartments affects energetic  
1467 communication in cardiomyocytes. Front Physiol 5:376.

1468 Breton S, Beaupré HD, Stewart DT, Hoeh WR, Blier PU (2007) The unusual system of doubly uniparental  
1469 inheritance of mtDNA: isn't one enough? Trends Genet 23:465-74.

1470 Brown GC (1992) Control of respiration and ATP synthesis in mammalian mitochondria and cells. Biochem J  
1471 284:1-13.

1472 Calvo SE, Klauser CR, Mootha VK (2016) MitoCarta2.0: an updated inventory of mammalian mitochondrial  
1473 proteins. Nucleic Acids Research 44:D1251-7.

1474 Calvo SE, Julien O, Clauser KR, Shen H, Kamer KJ, Wells JA, Mootha VK (2017) Comparative analysis of  
1475 mitochondrial N-termini from mouse, human, and yeast. Mol Cell Proteomics 16:512-23.

1476 Campos JC, Queliconi BB, Bozi LHM, Bechara LRG, Dourado PMM, Andres AM, Jannig PR, Gomes KMS,  
1477 Zambelli VO, Rocha-Resende C, Guatimosim S, Brum PC, Mochly-Rosen D, Gottlieb RA, Kowaltowski AJ,  
1478 Ferreira JCB (2017) Exercise reestablishes autophagic flux and mitochondrial quality control in heart failure.  
1479 Autophagy 13:1304-317.

1480 Canton M, Luvisetto S, Schmehl I, Azzone GF (1995) The nature of mitochondrial respiration and  
1481 discrimination between membrane and pump properties. Biochem J 310:477-81.

1482 Chance B, Williams GR (1955a) Respiratory enzymes in oxidative phosphorylation. I. Kinetics of oxygen  
1483 utilization. J Biol Chem 217:383-93.

1484 Chance B, Williams GR (1955b) Respiratory enzymes in oxidative phosphorylation: III. The steady state. J Biol  
1485 Chem 217:409-27.

1486 Chance B, Williams GR (1955c) Respiratory enzymes in oxidative phosphorylation. IV. The respiratory chain. J  
1487 Biol Chem 217:429-38.

- 1488 Chance B, Williams GR (1956) The respiratory chain and oxidative phosphorylation. *Adv Enzymol Relat Subj*  
1489 *Biochem* 17:65-134.
- 1490 Cobb LJ, Lee C, Xiao J, Yen K, Wong RG, Nakamura HK, Mehta HH, Gao Q, Ashur C, Huffman DM, Wan J,  
1491 Muzumdar R, Barzilai N, Cohen P (2016) Naturally occurring mitochondrial-derived peptides are age-  
1492 dependent regulators of apoptosis, insulin sensitivity, and inflammatory markers. *Aging (Albany NY)* 8:796-  
1493 809.
- 1494 Cohen ER, Cvitas T, Frey JG, Holmström B, Kuchitsu K, Marquardt R, Mills I, Pavese F, Quack M, Stohner J,  
1495 Strauss HL, Takami M, Thor HL (2008) Quantities, units and symbols in physical chemistry, IUPAC Green  
1496 Book, 3rd Edition, 2nd Printing, IUPAC & RSC Publishing, Cambridge.
- 1497 Cooper H, Hedges LV, Valentine JC, eds (2009) *The handbook of research synthesis and meta-analysis*. Russell  
1498 Sage Foundation.
- 1499 Coopersmith J (2010) *Energy, the subtle concept. The discovery of Feynman's blocks from Leibnitz to Einstein*.  
1500 Oxford University Press:400 pp.
- 1501 Cummins J (1998) Mitochondrial DNA in mammalian reproduction. *Rev Reprod* 3:172-82.
- 1502 Dai Q, Shah AA, Garde RV, Yonish BA, Zhang L, Medvitz NA, Miller SE, Hansen EL, Dunn CN, Price TM  
1503 (2013) A truncated progesterone receptor (PR-M) localizes to the mitochondrion and controls cellular  
1504 respiration. *Mol Endocrinol* 27:741-53.
- 1505 Divakaruni AS, Brand MD (2011) The regulation and physiology of mitochondrial proton leak. *Physiology*  
1506 (Bethesda) 26:192-205.
- 1507 Doerrier C, Garcia-Souza LF, Krumschnabel G, Wohlfarter Y, Mészáros AT, Gnaiger E (2018) High-Resolution  
1508 Fluorescence Respirometry and OXPHOS protocols for human cells, permeabilized fibres from small biopsies of  
1509 muscle and isolated mitochondria. *Methods Mol. Biol.* (in press)
- 1510 Doskey CM, van 't Erve TJ, Wagner BA, Buettner GR (2015) Moles of a substance per cell is a highly  
1511 informative dosing metric in cell culture. *PLOS ONE* 10:e0132572.
- 1512 Drahotka Z, Milerová M, Stieglerová A, Houstek J, Ostádal B (2004) Developmental changes of cytochrome c  
1513 oxidase and citrate synthase in rat heart homogenate. *Physiol Res* 53:119-22.
- 1514 Duarte FV, Palmeira CM, Rolo AP (2014) The role of microRNAs in mitochondria: small players acting wide.  
1515 *Genes (Basel)* 5:865-86.
- 1516 Ernster L, Schatz G (1981) Mitochondria: a historical review. *J Cell Biol* 91:227s-55s.
- 1517 Estabrook RW (1967) Mitochondrial respiratory control and the polarographic measurement of ADP:O ratios.  
1518 *Methods Enzymol* 10:41-7.
- 1519 Faber C, Zhu ZJ, Castellino S, Wagner DS, Brown RH, Peterson RA, Gates L, Barton J, Bickett M, Hagerty L,  
1520 Kimbrough C, Sola M, Bailey D, Jordan H, Elangbam CS (2014) Cardiolipin profiles as a potential  
1521 biomarker of mitochondrial health in diet-induced obese mice subjected to exercise, diet-restriction and  
1522 ephedrine treatment. *J Appl Toxicol* 34:1122-9.
- 1523 Fell D (1997) *Understanding the control of metabolism*. Portland Press.
- 1524 Garlid KD, Beavis AD, Ratkje SK (1989) On the nature of ion leaks in energy-transducing membranes. *Biochim*  
1525 *Biophys Acta* 976:109-20.
- 1526 Garlid KD, Semrad C, Zinchenko V. Does redox slip contribute significantly to mitochondrial respiration? In:  
1527 Schuster S, Rigoulet M, Ouhabi R, Mazat J-P, eds (1993) *Modern trends in biothermokinetics*. Plenum Press,  
1528 New York, London:287-93.
- 1529 Gerö D, Szabo C (2016) Glucocorticoids suppress mitochondrial oxidant production via upregulation of  
1530 uncoupling protein 2 in hyperglycemic endothelial cells. *PLoS One* 11:e0154813.
- 1531 Gnaiger E. Efficiency and power strategies under hypoxia. Is low efficiency at high glycolytic ATP production a  
1532 paradox? In: *Surviving Hypoxia: Mechanisms of Control and Adaptation*. Hochachka PW, Lutz PL, Sick T,  
1533 Rosenthal M, Van den Thillart G, eds (1993a) CRC Press, Boca Raton, Ann Arbor, London, Tokyo:77-109.
- 1534 Gnaiger E (1993b) Nonequilibrium thermodynamics of energy transformations. *Pure Appl Chem* 65:1983-2002.
- 1535 Gnaiger E (2001) Bioenergetics at low oxygen: dependence of respiration and phosphorylation on oxygen and  
1536 adenosine diphosphate supply. *Respir Physiol* 128:277-97.
- 1537 Gnaiger E (2009) Capacity of oxidative phosphorylation in human skeletal muscle. *New perspectives of*  
1538 *mitochondrial physiology*. *Int J Biochem Cell Biol* 41:1837-45.
- 1539 Gnaiger E (2014) *Mitochondrial pathways and respiratory control. An introduction to OXPHOS analysis*. 4th ed.  
1540 *Mitochondr Physiol Network* 19.12. Oroboros MiPNet Publications, Innsbruck:80 pp.
- 1541 Gnaiger E, Méndez G, Hand SC (2000) High phosphorylation efficiency and depression of uncoupled respiration  
1542 in mitochondria under hypoxia. *Proc Natl Acad Sci USA* 97:11080-5.
- 1543 Greggio C, Jha P, Kulkarni SS, Lagarrigue S, Broskey NT, Boutant M, Wang X, Conde Alonso S, Ofori E,  
1544 Auwerx J, Cantó C, Amati F (2017) Enhanced respiratory chain supercomplex formation in response to  
1545 exercise in human skeletal muscle. *Cell Metab* 25:301-11.
- 1546 Hinkle PC (2005) P/O ratios of mitochondrial oxidative phosphorylation. *Biochim Biophys Acta* 1706:1-11.
- 1547 Hofstadter DR (1979) Gödel, Escher, Bach: An eternal golden braid. A metaphorical fugue on minds and  
1548 machines in the spirit of Lewis Carroll. Harvester Press:499 pp.

- 1549 Illaste A, Laasmaa M, Peterson P, Vendelin M (2012) Analysis of molecular movement reveals latticelike  
1550 obstructions to diffusion in heart muscle cells. *Biophys J* 102:739-48.
- 1551 Jasienski M, Bazzaz FA (1999) The fallacy of ratios and the testability of models in biology. *Oikos* 84:321-26.
- 1552 Jepihhina N, Beraud N, Sepp M, Birkedal R, Vendelin M (2011) Permeabilized rat cardiomyocyte response  
1553 demonstrates intracellular origin of diffusion obstacles. *Biophys J* 101:2112-21.
- 1554 Klepinin A, Ounpuu L, Guzun R, Chekulayev V, Timohhina N, Tepp K, Shevchuk I, Schlattner U, Kaambre T  
1555 (2016) Simple oxygraphic analysis for the presence of adenylate kinase 1 and 2 in normal and tumor cells. *J*  
1556 *Bioenerg Biomembr* 48:531-48.
- 1557 Klingenberg M (2017) UCP1 - A sophisticated energy valve. *Biochimie* 134:19-27.
- 1558 Koit A, Shevchuk I, Ounpuu L, Klepinin A, Chekulayev V, Timohhina N, Tepp K, Puurand M, Truu L, Heck K,  
1559 Valvere V, Guzun R, Kaambre T (2017) Mitochondrial respiration in human colorectal and breast cancer  
1560 clinical material is regulated differently. *Oxid Med Cell Longev* 1372640.
- 1561 Komlódi T, Tretter L (2017) Methylene blue stimulates substrate-level phosphorylation catalysed by succinyl-  
1562 CoA ligase in the citric acid cycle. *Neuropharmacology* 123:287-98.
- 1563 Lane N (2005) Power, sex, suicide: mitochondria and the meaning of life. Oxford University Press:354 pp.
- 1564 Larsen S, Nielsen J, Neigaard Nielsen C, Nielsen LB, Wibrand F, Stride N, Schroder HD, Boushel RC, Helge  
1565 JW, Dela F, Hey-Mogensen M (2012) Biomarkers of mitochondrial content in skeletal muscle of healthy  
1566 young human subjects. *J Physiol* 590:3349-60.
- 1567 Lee C, Zeng J, Drew BG, Sallam T, Martin-Montalvo A, Wan J, Kim SJ, Mehta H, Hevener AL, de Cabo R,  
1568 Cohen P (2015) The mitochondrial-derived peptide MOTS-c promotes metabolic homeostasis and reduces  
1569 obesity and insulin resistance. *Cell Metab* 21:443-54.
- 1570 Lee SR, Kim HK, Song IS, Youm J, Dizon LA, Jeong SH, Ko TH, Heo HJ, Ko KS, Rhee BD, Kim N, Han J  
1571 (2013) Glucocorticoids and their receptors: insights into specific roles in mitochondria. *Prog Biophys Mol*  
1572 *Biol* 112:44-54.
- 1573 Leek BT, Mudaliar SR, Henry R, Mathieu-Costello O, Richardson RS (2001) Effect of acute exercise on citrate  
1574 synthase activity in untrained and trained human skeletal muscle. *Am J Physiol Regul Integr Comp Physiol*  
1575 280:R441-7.
- 1576 Lemieux H, Blier PU, Gnaiger E (2017) Remodeling pathway control of mitochondrial respiratory capacity by  
1577 temperature in mouse heart: electron flow through the Q-junction in permeabilized fibers. *Sci Rep* 7:2840.
- 1578 Lenaz G, Tioli G, Falasca AI, Genova ML (2017) Respiratory supercomplexes in mitochondria. In: Mechanisms  
1579 of primary energy trasduction in biology. M Wikstrom (ed) Royal Society of Chemistry Publishing, London,  
1580 UK:296-337.
- 1581 Margulis L (1970) Origin of eukaryotic cells. New Haven: Yale University Press.
- 1582 Meinild Lundby AK, Jacobs RA, Gehrig S, de Leur J, Hauser M, Bonne TC, Flück D, Dandanell S, Kirk N,  
1583 Kaech A, Ziegler U, Larsen S, Lundby C (2018) Exercise training increases skeletal muscle mitochondrial  
1584 volume density by enlargement of existing mitochondria and not de novo biogenesis. *Acta Physiol* 222,  
1585 e12905.
- 1586 Menshikova EV, Ritov VB, Fairfull L, Ferrell RE, Kelley DE, Goodpaster BH (2006) Effects of exercise on  
1587 mitochondrial content and function in aging human skeletal muscle. *J Gerontol A Biol Sci Med Sci* 61:534-  
1588 40.
- 1589 Menshikova EV, Ritov VB, Ferrell RE, Azuma K, Goodpaster BH, Kelley DE (2007) Characteristics of skeletal  
1590 muscle mitochondrial biogenesis induced by moderate-intensity exercise and weight loss in obesity. *J Appl*  
1591 *Physiol* (1985) 103:21-7.
- 1592 Menshikova EV, Ritov VB, Toledo FG, Ferrell RE, Goodpaster BH, Kelley DE (2005) Effects of weight loss  
1593 and physical activity on skeletal muscle mitochondrial function in obesity. *Am J Physiol Endocrinol Metab*  
1594 288:E818-25.
- 1595 Miller GA (1991) The science of words. Scientific American Library New York:276 pp.
- 1596 Mitchell P (1961) Coupling of phosphorylation to electron and hydrogen transfer by a chemi-osmotic type of  
1597 mechanism. *Nature* 191:144-8.
- 1598 Mitchell P (2011) Chemiosmotic coupling in oxidative and photosynthetic phosphorylation. *Biochim Biophys*  
1599 *Acta Bioenergetics* 1807:1507-38.
- 1600 Mogensen M, Sahlin K, Fernström M, Glinborg D, Vind BF, Beck-Nielsen H, Højlund K (2007) Mitochondrial  
1601 respiration is decreased in skeletal muscle of patients with type 2 diabetes. *Diabetes* 56:1592-9.
- 1602 Mohr PJ, Phillips WD (2015) Dimensionless units in the SI. *Metrologia* 52:40-7.
- 1603 Moreno M, Giacco A, Di Munno C, Goglia F (2017) Direct and rapid effects of 3,5-diiodo-L-thyronine (T2).  
1604 *Mol Cell Endocrinol* 7207:30092-8.
- 1605 Morrow RM, Picard M, Derbeneva O, Leipzig J, McManus MJ, Gouspillou G, Barbat-Artigas S, Dos Santos C,  
1606 Hepple RT, Murdock DG, Wallace DC (2017) Mitochondrial energy deficiency leads to hyperproliferation of  
1607 skeletal muscle mitochondria and enhanced insulin sensitivity. *Proc Natl Acad Sci U S A* 114:2705-10.
- 1608 Murley A, Nunnari J (2016) The emerging network of mitochondria-organelle contacts. *Mol Cell* 61:648-53.

- 1609 National Academies of Sciences, Engineering, and Medicine (2018) International coordination for science data  
 1610 infrastructure: Proceedings of a workshop—in brief. Washington, DC: The National Academies Press. doi:  
 1611 <https://doi.org/10.17226/25015>.
- 1612 Paradies G, Paradies V, De Benedictis V, Ruggiero FM, Petrosillo G (2014) Functional role of cardiolipin in  
 1613 mitochondrial bioenergetics. *Biochim Biophys Acta* 1837:408-17.
- 1614 Pesta D, Gnaiger E (2012) High-Resolution Respirometry. OXPHOS protocols for human cells and  
 1615 permeabilized fibres from small biopsies of human muscle. *Methods Mol Biol* 810:25-58.
- 1616 Pesta D, Hoppel F, Macek C, Messner H, Faulhaber M, Kobel C, Parson W, Burtcher M, Schocke M, Gnaiger  
 1617 E (2011) Similar qualitative and quantitative changes of mitochondrial respiration following strength and  
 1618 endurance training in normoxia and hypoxia in sedentary humans. *Am J Physiol Regul Integr Comp Physiol*  
 1619 301:R1078–87.
- 1620 Price TM, Dai Q (2015) The role of a mitochondrial progesterone receptor (PR-M) in progesterone action.  
 1621 *Semin Reprod Med* 33:185-94.
- 1622 Puchowicz MA, Varnes ME, Cohen BH, Friedman NR, Kerr DS, Hoppel CL (2004) Oxidative phosphorylation  
 1623 analysis: assessing the integrated functional activity of human skeletal muscle mitochondria – case studies.  
 1624 *Mitochondrion* 4:377-85. Puntschart A, Claassen H, Jostardt K, Hoppeler H, Billeter R (1995) mRNAs of  
 1625 enzymes involved in energy metabolism and mtDNA are increased in endurance-trained athletes. *Am J*  
 1626 *Physiol* 269:C619-25.
- 1627 Quiros PM, Mottis A, Auwerx J (2016) Mitonuclear communication in homeostasis and stress. *Nat Rev Mol*  
 1628 *Cell Biol* 17:213-26.
- 1629 Rackham O, Mercer TR, Filipovska A (2012) The human mitochondrial transcriptome and the RNA-binding  
 1630 proteins that regulate its expression. *WIREs RNA* 3:675–95.
- 1631 Reichmann H, Hoppeler H, Mathieu-Costello O, von Bergen F, Pette D (1985) Biochemical and ultrastructural  
 1632 changes of skeletal muscle mitochondria after chronic electrical stimulation in rabbits. *Pflugers Arch* 404:1-  
 1633 9.
- 1634 Renner K, Amberger A, Konwalinka G, Gnaiger E (2003) Changes of mitochondrial respiration, mitochondrial  
 1635 content and cell size after induction of apoptosis in leukemia cells. *Biochim Biophys Acta* 1642:115-23.
- 1636 Rich P (2003) Chemiosmotic coupling: The cost of living. *Nature* 421:583.
- 1637 Rostovtseva TK, Sheldon KL, Hassanzadeh E, Monge C, Saks V, Bezrukov SM, Sackett DL (2008) Tubulin  
 1638 binding blocks mitochondrial voltage-dependent anion channel and regulates respiration. *Proc Natl Acad Sci*  
 1639 *USA* 105:18746-51.
- 1640 Rustin P, Parfait B, Chretien D, Bourgeron T, Djouadi F, Bastin J, Rötig A, Munnich A (1996) Fluxes of  
 1641 nicotinamide adenine dinucleotides through mitochondrial membranes in human cultured cells. *J Biol Chem*  
 1642 271:14785-90.
- 1643 Saks VA, Veksler VI, Kuznetsov AV, Kay L, Sikk P, Tiivel T, Tranqui L, Olivares J, Winkler K, Wiedemann F,  
 1644 Kunz WS (1998) Permeabilised cell and skinned fiber techniques in studies of mitochondrial function in  
 1645 vivo. *Mol Cell Biochem* 184:81-100.
- 1646 Salabei JK, Gibb AA, Hill BG (2014) Comprehensive measurement of respiratory activity in permeabilized cells  
 1647 using extracellular flux analysis. *Nat Protoc* 9:421-38.
- 1648 Sazanov LA (2015) A giant molecular proton pump: structure and mechanism of respiratory complex I. *Nat Rev*  
 1649 *Mol Cell Biol* 16:375-88.
- 1650 Schneider TD (2006) Claude Shannon: biologist. The founder of information theory used biology to formulate  
 1651 the channel capacity. *IEEE Eng Med Biol Mag* 25:30-3.
- 1652 Schönfeld P, Dymkowska D, Wojtczak L (2009) Acyl-CoA-induced generation of reactive oxygen species in  
 1653 mitochondrial preparations is due to the presence of peroxisomes. *Free Radic Biol Med* 47:503-9.
- 1654 Schultz J, Wiesner RJ (2000) Proliferation of mitochondria in chronically stimulated rabbit skeletal muscle--  
 1655 transcription of mitochondrial genes and copy number of mitochondrial DNA. *J Bioenerg Biomembr* 32:627-  
 1656 34.
- 1657 Spejjer D (2016) Being right on Q: shaping eukaryotic evolution. *Biochem J* 473:4103-27.
- 1658 Sugiura A, Mattie S, Prudent J, McBride HM (2017) Newly born peroxisomes are a hybrid of mitochondrial and  
 1659 ER-derived pre-peroxisomes. *Nature* 542:251-4.
- 1660 Simson P, Jephthina N, Laasmaa M, Peterson P, Birkedal R, Vendelin M (2016) Restricted ADP movement in  
 1661 cardiomyocytes: Cytosolic diffusion obstacles are complemented with a small number of open mitochondrial  
 1662 voltage-dependent anion channels. *J Mol Cell Cardiol* 97:197-203.
- 1663 Stucki JW, Ineichen EA (1974) Energy dissipation by calcium recycling and the efficiency of calcium transport  
 1664 in rat-liver mitochondria. *Eur J Biochem* 48:365-75.
- 1665 Tonkonogi M, Harris B, Sahlin K (1997) Increased activity of citrate synthase in human skeletal muscle after a  
 1666 single bout of prolonged exercise. *Acta Physiol Scand* 161:435-6.
- 1667 Vamecq J, Schepers L, Parmentier G, Mannaerts GP (1987) Inhibition of peroxisomal fatty acyl-CoA oxidase by  
 1668 antimycin A. *Biochem J* 248:603-7.



- 1669 Waczulikova I, Habodaszova D, Cagalinec M, Ferko M, Ulicna O, Mateasik A, Sikurova L, Ziegelhöffer A  
1670 (2007) Mitochondrial membrane fluidity, potential, and calcium transients in the myocardium from acute  
1671 diabetic rats. *Can J Physiol Pharmacol* 85:372-81.
- 1672 Wagner BA, Venkataraman S, Buettner GR (2011) The rate of oxygen utilization by cells. *Free Radic Biol Med*  
1673 51:700-712.
- 1674 Wang H, Hiatt WR, Barstow TJ, Brass EP (1999) Relationships between muscle mitochondrial DNA content,  
1675 mitochondrial enzyme activity and oxidative capacity in man: alterations with disease. *Eur J Appl Physiol*  
1676 *Occup Physiol* 80:22-7.
- 1677 Watt IN, Montgomery MG, Runswick MJ, Leslie AG, Walker JE (2010) Bioenergetic cost of making an  
1678 adenosine triphosphate molecule in animal mitochondria. *Proc Natl Acad Sci U S A* 107:16823-7.
- 1679 Weibel ER, Hoppeler H (2005) Exercise-induced maximal metabolic rate scales with muscle aerobic capacity. *J*  
1680 *Exp Biol* 208:1635-44.
- 1681 White DJ, Wolff JN, Pierson M, Gemmell NJ (2008) Revealing the hidden complexities of mtDNA inheritance.  
1682 *Mol Ecol* 17:4925-42.
- 1683 Wikström M, Hummer G (2012) Stoichiometry of proton translocation by respiratory complex I and its  
1684 mechanistic implications. *Proc Natl Acad Sci U S A* 109:4431-6.
- 1685 Willis WT, Jackman MR, Messer JI, Kuzmiak-Glancy S, Glancy B (2016) A simple hydraulic analog model of  
1686 oxidative phosphorylation. *Med Sci Sports Exerc* 48:990-1000.
- 1687